Aus der Klinik für Audiologie und Phoniatrie
der Medizinischen Fakultät Charité – Universitätsmedizin Berlin

DISSERTATION

Probabilistic tractography of the neural language network in deaf and hearing adults

Probabilistische Traktographie des neuronalen Sprachnetzwerks bei tauben und hörenden Erwachsenen

zur Erlangung des akademischen Grades
Doctor rerum medicinalium (Dr. rer. medic.)

vorgelegt der Medizinischen Fakultät
Charité – Universitätsmedizin Berlin

von

Theresa Finkl, M.Sc. Integrative Neuroscience

aus Augsburg

Datum der Promotion: 18.12.2020

Diese Dissertation basiert auf folgendem Artikel:

Theresa Finkl, Anja Hahne, Angela D Friederici, Johannes Gerber, Dirk Mürbe, Alfred Anwander, **Language Without Speech: Segregating Distinct Circuits in the Human Brain**, *Cerebral Cortex*, Volume 30, Issue 2, February 2020, Pages 812–823, https://doi.org/10.1093/cercor/bhz128, *online publiziert August 2019*

INHALTSVERZEICHNIS

ABKÜRZUNGEN

AD	Axial diffusivity
AF	Arcuate fasciculus
BA	Brodmann area
CI	Cochlear implant
dB	Decibel
DIVA	Directions into velocities of articulators
dMRI	Diffusion-weighted magnetic resonance imaging
DTI	Diffusion tensor imaging
FA	Fractional anisotropy
Hz	Hertz
LL	Lateral lemniscus
MD	Mean diffusivity
MRI	Magnetic resonance imaging
RD	Radial diffusivity
ROI	Region of interest
SLF	Superior longitudinal fasciculus
SMA	Supplementary motor area
STG	Superior temporal gyrus
WHO	World Health Organization

1 ABSTRAKT

1.1 Deutsch

In der Geschichte der Sprachforschung wurde Sprache ("language") lange mit gesprochener Sprache, bzw. dem Sprechen ("speech") gleichgesetzt, obwohl das Sprechen nur eine Form ist, Sprache auszudrücken. Dies kann genauso über das Schreiben oder das Gebärden erfolgen. Es gibt zunehmende neurophysiologische Evidenz für diese Theorie der getrennten Verarbeitung von Sprache und Sprechen. Diese geht von einem zentralen Netzwerk ("core language network") aus, das syntaktische und semantische Aspekte von Sprache verarbeitet, und damit eng verbundenen Input- und Output-Elementen auf sensorisch-motorischer Ebene.

Zudem deuten Studien mit tauben Teilnehmenden darauf hin, dass die semantische und syntaktische Verarbeitung von Gebärdensprache in den gleichen Regionen des perisylvischen Sprachnetzwerks erfolgt wie bei gesprochener Sprache. Hierbei sind nicht nur die relevanten Areale, sondern auch die verbindenden Faserbündel in das wissenschaftliche Interesse gerückt. So weiß man aus Diffusions-Tensor-Imaging (DTI)-Studien, dass auditorische Faserbahnen bei tauben Menschen Veränderungen bestimmter Parameter aufweisen, die Rückschlüsse auf verringerte Myelinisierung und Faserdichte zulassen. Basierend auf diesen Erkenntnissen lautet die zentrale Frage meiner Arbeit: Lässt sich die bisher theoretisch und funktionell beschriebene getrennte Verarbeitung von Sprache und Sprechen auch strukturell untermauern?

Dazu habe ich mittels probabilistischer Traktographie die Konnektivität von sechs sprach- und sprechrelevanten Regionen pro Hemisphäre bei zehn tauben und zehn hörenden Teilnehmenden untersucht. Die Gruppenvergleiche zeigten eine verringerte Konnektivitätswahrscheinlichkeit in den Input/Output-Trakten der tauben Teilnehmenden, nicht aber in ihrem zentralen Sprachnetzwerk. Damit unterstützen die Ergebnisse die Theorie der getrennten Verarbeitung von Sprache und Sprechen und ergänzen die Aufteilung in zentrales Sprachnetzwerk und Input/Output-System um den strukturellen Aspekt. Zudem unterstützen die Ergebnisse auch die Hypothese, dass das zentrale Sprachnetzwerk modalitätsunabhängig ist und sich adäquat entwickelt, auch wenn der Sprachinput über Gebärdensprache erfolgt.

1.2 Englisch

In the history of language research, language and speech have long been equated, although speech only represents one possibility of externalizing language. This can be achieved just as well by writing or signing. Increasing neurophysiological evidence supports this theory of separate processing of speech and language, assuming a division into a core language network, that processes syntactic and semantic aspects of language, and a closely linked sensory-motor input/output system.

In addition, studies involving deaf participants point to a recruitment of similar perisylvian regions for signed and spoken language. Apart from these brain areas, their connecting pathways have progressively attracted scientific interest. Diffusion tensor imaging (DTI)-studies have shown alterations of different diffusion parameters indicating reduced myelination and fiber density in auditory pathways of deaf participants. Based on these findings, the central question of my work is: Can the theoretically proposed and functionally described separation of speech and language processing be corroborated on a structural level?

To this end, I employed probabilistic fiber tracking to investigate the connectivity of six language- and speech-relevant areas in both hemispheres of ten deaf and ten hearing participants. The group comparisons showed reduced connection probability in the input/output tracts, but not in the core language network of the deaf participants. Thus, the results support the theory of separated language and speech processing in the brain and add structural evidence for the division into a core language network and an input/output system. Furthermore, they support the idea of a modality-independent language network that can develop normally with purely vision-based sign language input.

I think, therefore I am. – René Descartes

I speak, therefore I am. – Andrea Moro

2 MANTELTEXT

Humans have been using language for millennia. This fascinating cognitive capacity allowed us to become interested in its own evolution, underlying principles, and mechanisms. Language has been challenging scientists from various disciplines including philosophy, anthropology, linguistics, psychology, medicine and neuroscience for centuries and continues to be investigated intensely, raising questions like: What is language? How do we speak? How did language(s) evolve? How do they differ? How can we treat language disorders? Which regions in the brain are involved in language processing? How do children learn to speak?

We use and acquire (our maternal) language so naturally that some researchers claim that learning language is what we are born to (Friederici 2017). Language is the most important basis for our communication, allowing us to express our thoughts and emotions, to talk about past and future events, and to write very specifically about its own abstract concepts – all with a finite set of characters (or phonemes) that we can combine to words and an unlimited number of phrases.

However, language itself is of no use for communication without expressing it for a recipient. In direct communication, we achieve this by speaking. When speaking is no (viable) option, our innate urge for social interaction leads to the development of other forms of communication. In some regions of the world, people have developed whistled languages that cover distances of several hundred meters. This allows communication between members of a community living on different flanks of a valley, for example (Meyer 2008). When hearing is severely impaired, however, auditory-vocal language expression is abandoned altogether in favor of visual-gestural communication. In communities with a high number of deaf individuals, sign languages and deaf cultures have evolved, enriching the linguistic diversity substantially.

The special combination of language without speech in deaf signers has been investigated extensively and has added insights into language processing in the brain. Building on these previous results, this work aims at contributing one piece to the puzzle of understanding the neuroanatomical groundings of language and speech processing.

The motivation for this is twofold: First, understanding how language and speech are represented in the brain is the basis for diagnosis and therapy of neuropsychological conditions related to language processing, such as aphasia, apraxia, dysarthria and others. Second, the brain and its incredible capacities have always fascinated me – with language being a wonderful playground for the creative mind and an extensive experimental ground for the scientific one that has guided this work.

The main part begins with a brief overview of hearing loss and deafness (chapter 2.1). Providing a theoretical basis for the study, different aspects of language processing are then discussed along with their anatomical representation in the brain (chapter 2.2). Differences between spoken and signed language processing, which have guided the development of the hypotheses are addressed (chapter 2.3). Probabilistic tractography is described in order to set a comprehensible basis for the results (chapter 2.4). The findings are discussed subsequently with regard to their implications (chapter 2.5), before considerations for future research are presented (chapter 2.6).

2.1 Classification of hearing loss and deafness

According to a recent review, 5 % of the world's population suffer from disabling hearing loss (Sheffield and Smith 2019), referring to hearing loss in the better ear greater than 40 decibel (dB) in adults and greater than 30 dB in children (World Health Organization 2020). Regarding Germany, a nationwide assessment targeting the prevalence of hearing disorders is not available to date. However, a study in two regions in Germany with more than 3000 participants suggests that 16 % of the German population have a hearing loss greater than 25 dB (von Gablenz et al. 2017). Hearing loss and deafness can be classified regarding different parameters. The most relevant ones for this study are severity, age of onset, and affected structures, which will be briefly specified in the following sections.

2.1.1 Severity of hearing loss

The World Health Organization (WHO) distinguishes four grades of hearing loss, as summarized in Table 1. Hearing loss up to 25 dB averaged over speech-relevant frequencies (usually 500 Hertz (Hz), 1000 Hz, 2000 Hz, 4000 Hz) is classified as normal hearing without functional impairment.

Table 1: Grades of hearing loss and according functional impairment.
Modified from WHO | Grades of hearing impairment (2020)

Amount of hearing loss	Grade of hearing loss	Functional impairment
26-40 dB	Mild	Difficulties hearing soft or distant speech or speech against background noise
41-60 dB	Moderate	Difficulties hearing regular speech
61-80 dB	Severe	Incapable of hearing most conversational speech; only loud sounds are heard
≥81 dB	Profound	Even loud sounds are not heard, but may be perceived as vibrations

2.1.2 Age at onset of hearing loss

Hearing loss present at birth is uniformly described as congenital hearing loss. About 0.12 % of all infants born in Germany display congenital, persistent and bilateral deafness (Spormann-Lagodzinski et al. 2003). The terms “prelingual”, “perilingual” and “postlingual” refer to the age of onset of deafness with regard to language acquisition. Prelingual hearing loss includes all types of hearing loss occurring before language acquisition (also congenital hearing loss) and postlingual hearing loss describes hearing loss after language acquisition is completed (Shearer et al. 1993). When hearing loss occurs during the process of language acquisition, sometimes the term perilingual hearing loss is used.

Since the introduction of the newborn hearing screening, infants suffering from hearing loss can be diagnosed and treated earlier (Weichbold et al. 2005), raising the chances for successful speech comprehension with hearing aids or cochlear implants by decreasing the duration of auditory deprivation (Kral and Sharma 2012). Before the newborn hearing screening was introduced, patients were often diagnosed later during childhood, even though their hearing loss had been present before. Retrospective classification of these deaf and hearing-impaired adults, who were not screened at birth, has to rely on old (and often incomplete) medical records and subjective patients’ reports on their hearing history. Clinically, postlingual hearing loss can be distinguished well from pre- and perilingual hearing loss, while pre- and perilingual hearing loss often appear more similar and are sometimes hard to differentiate retrospectively when no early diagnosis has been made.

2.1.3 Affected Structures

Hearing loss can be caused by disruptions at any stage along the auditory pathway from the external ear to the auditory cortex in the brain. The site of damage determines the quality of hearing loss and is an important criterion for further treatment. Four different types are distinguished.

Conductive hearing loss

Any disruption of sound transmission occurring in the external or middle ear is classified as conductive hearing loss. A ruptured eardrum can be surgically restored and different types of bone conduction and middle ear implants are available for treatment of middle-ear malfunction.

Sensory hearing loss

Absent or diminished signal conversion in the Organ of Corti, such as damage to the hair cells caused by noise exposure, malformation, trauma or ototoxic drugs is termed sensory hearing loss. Sensory hearing loss is permanent, as human cochlear hair cells do not regrow. To date, hearing aids and cochlear implants are the state-of-the-art intervention for sensory hearing loss.

Neural hearing loss

In neural hearing loss, the cochlear nerve is affected, while external and internal ear are intact. Thus, the signal cannot be transmitted to the brain. Depending on the cause of cochlear nerve malfunction, such as tumors or lesions, treatment options range from removal of the tumor to auditory brainstem implants passing the signal directly to the cochlear nucleus in the brainstem. Hearing deficits related to the cochlea (sensory) or the cochlear nerve (neural) are often grouped together and referred to as sensorineural hearing loss.

Central hearing loss

Central hearing loss occurs in the central nervous system and can be caused by tumors, lesions or other damage between brainstem and higher auditory areas. This can lead to phenomena like auditory agnosia (Slevc and Shell 2015).

The deaf participants in this study displayed permanent, bilateral, prelingual and profound sensorineural deafness with average hearing loss of more than 95 dB in the better ear at speech-relevant frequencies.

2.2 The language network

2.2.1 Language perception: from ear to auditory cortex

Before the brain can extract meaning from speech sounds, the sound waves travel from the ear to the auditory cortex, being transferred from a physical to an electric signal, relayed at several stages, filtered, and enriched with available environmental and other relevant information. The following abstract describes the most important stages of the input system responsible for speech perception with a focus on the segments from the auditory nerve upwards.

When we listen to someone who is speaking to us, the sound waves reach our ear(s) and move the tympanic membrane that separates the external ear from the air filled middle-ear cavity. Directly attached to the tympanic membrane, the three interconnected middle-ear ossicles – malleus, incus, and stapes – transmit and amplify the sound towards the oval window that marks the boundary to the cochlea in the inner ear. The cochlea, a fluid-filled tube in the shape of a snail's shell, contains the organ of Corti, where the mechanical sound wave is turned into a neural signal. This is achieved by the sensory hair cells that share a synaptic connection with the endings of the cochlear nerve fibers. An important feature of the cochlea is its tonotopy: high frequencies are represented near the oval window and low frequencies near the tip of the cochlea, allowing for a first frequency analysis. This tonotopic organization is maintained throughout the whole auditory pathway up to the auditory cortex.

As depicted in Figure 1 on the following page (Pickles 2015), the cochlear nerve transmits the information to the ipsilateral cochlear nuclei (anteroventral, posteroventral and dorsal cochlear nucleus), where a basic frequency and timing analysis takes place. Here, the signal takes three different processing paths, each responsible for a particular aspect of the highly complex task of auditory object recognition and synthesis with the environment.

Localization of sound is processed via the ventral stream. The signal from the anteroventral cochlear nucleus is conveyed to bilateral superior olivary complexes consisting of medial and lateral superior olive, while the crossing fibers are relayed on the way in the medial nucleus of the trapezoid body. The superior olivary complex is the first

station receiving information from both ears. This enables a rapid analysis of interaural time (in the medial superior olive) and intensity (in the lateral superior olive) differences that are the basis for directional hearing and sound localization. From the medial superior olive, the signal is passed on to the ipsilateral inferior colliculus via the lateral lemniscus (LL), while fibers from the lateral superior olive join the contralateral LL to the inferior colliculus, both passing through the dorsal nucleus of the LL, where a more fine-grained localization analysis takes place.

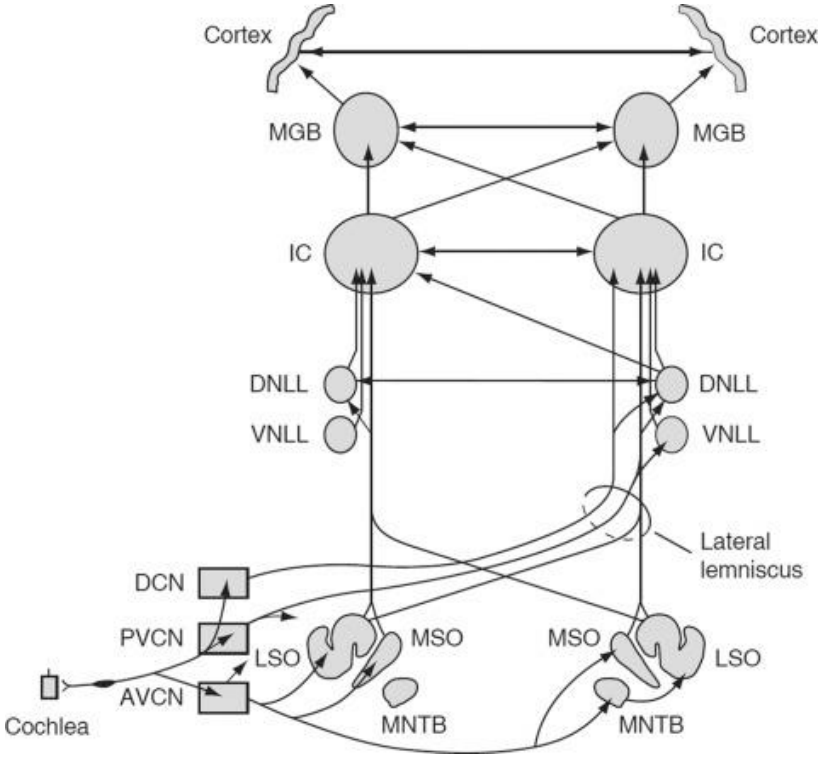

Figure 1: Simplified scheme of the ascending auditory pathways with the most important relay stations and their connections. Abbreviations in order of appearance in the text. AVCN: anteroventral cochlear nucleus; PVCN: posteroventral cochlear nucleus; DCN: dorsal cochlear nucleus; LSO: lateral superior olive; MSO: medial superior olive; MNTB: medial nucleus of the trapezoid body; VNLL: ventral nucleus of the lateral lemniscus DNLL: dorsal nucleus of the lateral lemniscus; IC: inferior colliculus; MGB: medial geniculate body. *Figure reprinted from Pickles (2015) with permission from Elsevier*[1] *and Brill*[2].

[1] Pickles JO. 2015. Chapter 1 - Auditory pathways: anatomy and physiology. In: Aminoff MJ, Boller F, Swaab DF, editors. Handbook of Clinical Neurology. The Human Auditory System. Elsevier. p. 3–25. Copyright 2015.

[2] Pickles JO. 2013. An introduction to the physiology of hearing. 4th ed. Leiden: Brill. Copyright 2013.

In the dorsal stream, starting from dorsal and posteroventral cochlear nuclei, a complex sound analysis is conducted, taking into account spectral and temporal patterns of the auditory stimulus. The vast majority of fibers cross via the LL to the contralateral ventral nucleus of the LL and continue further to the inferior colliculus.

The non-lemniscal pathway runs in parallel to the LL and is strongly interconnected with it. This stream integrates multisensory information and emotions and is important for reflexes to auditory stimuli (not shown in the figure).

In the inferior colliculus, the streams converge and the signal is further analyzed and then being passed on to the medial geniculate bodies in the thalamus before reaching the auditory cortices via the acoustic radiation, being enriched with information from the contralateral stream at every station upwards. In addition, a complex top-down organized system modulates and affects the bottom-up auditory processing described earlier. By the time the auditory information reaches the auditory cortex, it has already been analyzed intensely, filtered and connected with other available information on the way.

Much of what is known about the auditory cortex is based on animal studies including rats, gerbils, cats and macaques, all displaying a primary “core” region and adjacent secondary “belt” and “parabelt” regions that are in themselves tonotopically organized (Hackett 2015). In humans, the exact location, extent and nomenclature is still under debate. However, a primary region in Heschl’s Gyrus, corresponding to Brodmann area 41 (BA41), and neighboring secondary areas in BA52, BA22, and BA42 in the superior temporal cortex are widely accepted as cortical processing nodes for auditory stimuli. These regions are heavily interconnected within the temporal cortex, extending to the inferior parietal lobule (Häkkinen and Rinne 2018), ensuring both hierarchical and parallel processing of the auditory stimuli.

In addition to these short connections, long-range commissural fiber tracts connect left and right auditory cortices via the posterior part of the corpus callosum. The left auditory cortex is specialized in processing segmental aspects of speech signals, i.e. consonants and vowels, while the right auditory cortex is more responsive to supra-segmental changes such as pitch, duration and loudness. Strong interhemispheric pathways are therefore of crucial importance for the rapid integration of the two hemispheres’ individual analyses (Hickok

and Poeppel 2007). This applies in particular to the decoding of complex speech signals, as a change in intonation can alter the meaning of an utterance altogether, for example turning a phrase like “She finished writing her thesis.” from an appreciatory statement into a disbelieving question. Further in-depth processing of the speech signal occurs in the auditory cortices and beyond, in order to extract meaning and prepare an appropriate response or action, if necessary.

2.2.2 Language processing: the core language network

The mere perception of speech requires sensory processing and does not require the core language network. Comprehension of speech, however, can only occur with a functioning language network that processes the perceived speech input accordingly, thus needing an interplay between sensory input and core language network. This dissociation between perception and comprehension becomes apparent in auditory verbal agnosia, a rare phenomenon caused by damage in higher auditory and language-related cortical regions, that are not yet clearly defined. Patients suffering from this condition have normal hearing and can speak, read, write, and perceive speech, yet they are unable to understand what is being said. In its pure form, identification of environmental sounds is not affected, which is why this form of agnosia is also termed “word deafness” (Slevc and Shell 2015).

Our understanding of the core language network has evolved from the historical model (Geschwind 1970) of two major nodes – Broca’s area and Wernicke’s area – connected by the arcuate fasciculus (AF) to a larger and more complex network. There is now consensus on a left-lateralized network[3] composed of dorsal and ventral pathways that are centered around the Sylvian fissure (Friederici et al. 2017), comparable to the dual-stream model in the visual domain (Ungerleider and Mishkin 1982).

Figure 2 on the following page shows schematized and simplified the four main fiber tracts connecting frontal, parietal and temporal regions that are involved in language processing.

[3] This is valid for the vast majority of people. Interestingly, some people have an ambilateral language network, while a strong lateralization to the right seems to occur only in a small fraction of left-handers (Mazoyer et al. 2014).

Dorsal to the Sylvian fissure, the superior longitudinal fasciculus (SLF) between the posterior superior temporal gyrus (STG) and the premotor cortex in the frontal lobe is suggested to process auditory-motor mapping (Hickok and Poeppel 2007). In close proximity and partly in parallel, the AF follows the same trajectory between posterior STG and frontal cortex, but extends more frontally to BA44 in the inferior frontal gyrus and further temporally to the posterior middle temporal gyrus (Anwander et al. 2007).

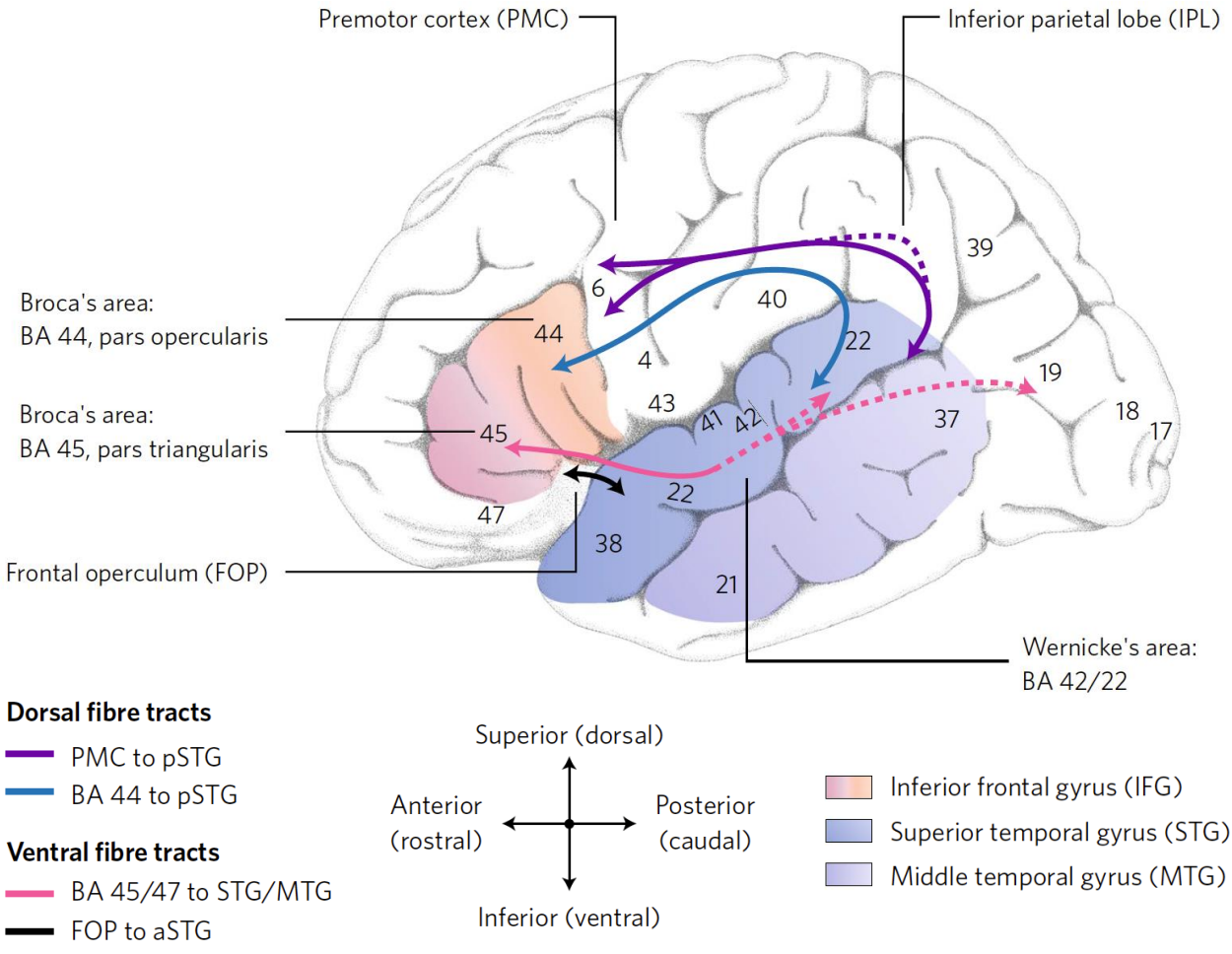

Figure 2: Schematic and simplified view of the core language network. *Figure adapted from Friederici et al. (2017) with permission from Springer Nature*[4] *and The American Physiological Society*[5].

[4] Friederici AD, Chomsky N, Berwick RC, Moro A, Bolhuis JJ. 2017. Language, mind and brain. Nat Hum Behav. 1:713–722. Copyright 2017.

[5] Friederici AD. 2011. The Brain Basis of Language Processing: From Structure to Function. Physiological Reviews. 91:1357–1392. Copyright 2011.

BA44 in Broca's area is the key region for complex syntax processing (Friederici et al. 2000), which is reflected in the function of the AF. Further evidence for the functional distinction of the two pathways is provided by the finding that the SLF targeting BA6 is already present and well myelinated at birth, while the connection towards BA44 only matures with language acquisition (Perani et al. 2011). Supporting the AF's essential role in complex syntax processing, this tract appears less pronounced and does not extend to BA44 and beyond the posterior STG in non-human primates (Rilling et al. 2008). Furthermore, the primates are unable to acquire complex syntactic rules (Fitch and Hauser 2004), underlining the idea that language is fundamentally human (Friederici 2017).

The main language fiber tracts ventral to the Sylvian fissure are the short, hook-shaped uncinate fasciculus, linking the frontal operculum to the anterior STG, and the inferior fronto-occipital fasciculus. This pathway connects BA45/BA47, the anterior portion of Broca's area, to the temporal, parietal, and occipital cortex and is mainly involved in semantic processing. The uncinate fasciculus' exact function in language processing remains to be determined (for a review see Friederici et al. 2017).

As described earlier, the left hemisphere is specialized in detecting high-temporal auditory signal changes, which is important for the differentiation of phonemes in spoken language. The right hemisphere contributes more to the processing of spectral variations of auditory stimuli, which could already be shown in newborns (Telkemeyer et al. 2009). The processing of spectral variations is important for extracting information from prosodic aspects of speech that add context to the words being said, such as emotional state or intention of the speaker, which in turn influences our reaction to the things we hear. Anatomically, prosodic processing seems to be located in a right-hemispheric fronto-temporal network, corresponding to the left-lateralized network for syntactic and semantic language processing (Sammler et al. 2015; Seydell-Greenwald et al. 2020).

We have no difficulty understanding language when prosodic information is not available, for example when we read texts that convey purely factual information. However, when personal relationships, dialogue and emotions come into play, syntactic and semantic information alone are sometimes not sufficient. Cues like "she said ironically" add valuable

insight to written dialogue and prevent misunderstandings. These cues do not necessarily need to be written words – emoticons in text messages are popular for a good reason.

Successful and rapid processing of speech relies on the integration of all three elements: syntax, semantics, and prosody, requiring interhemispheric connections of auditory- and language-related areas. As meaning has to be extracted from a continuous stream of sound, speech comprehension requires auditory attention, which has been attributed to regions in the right superior parietal and frontal cortices (Zatorre et al. 1999) within the global attention network. In addition, working memory, spanning a large network for a variety of higher cognitive processes (D'Esposito and Postle 2015), is – and this is particularly true for syntactically complex sentences like this one – an important prerequisite not only for comprehension, but also for the production of both spoken and written language, involving the left parietal cortex as key region for sentence processing (Meyer et al. 2013).

2.2.3 Language production: from response initiation to motor command

The interplay between the sensory input system and the core language network is essential for extracting relevant information from spoken language. The same principle can be applied to the production of speech: close interaction of the core language network and the motor output system are the basis for the generation of meaningful utterances. In addition to the neural network, speech production requires the interplay between respirational, oropharyngeal and facial muscles to create the speech sounds. In order to constantly monitor articulation and phonation, the respective circuits are coupled to the auditory input and proprioceptive system, resulting in a vast cortical and subcortical network involved in speech production. Guenther proposed a comprehensive neuro-computational model of speech production (Guenther 1995): the DIVA model (DIVA: directions into velocities of articulators). It has been tested in a variety of neuroimaging and clinical settings and has recently been refined and extended with regard to the neuroanatomical substrates reported to support the respective functions (Kearney and Guenther 2019). Figure 3 schematically shows the proposed nodes and connections.

According to this model, whenever speech production is planned, neurons in the left ventral premotor cortex become activated, where every learned speech sound is represented. The speaking process is then initiated via a cortico-basal ganglia-thalamic loop including the supplementary motor area (SMA). This leads to an activation of neurons in the ventral motor cortex of both hemispheres. In addition, neurons in the ventral premotor cortex also project to the ventral motor cortex neurons directly and via a second pathway passing the pons, cerebellum and thalamus, eventually resulting in a bilateral motor command for the articulatory muscles.

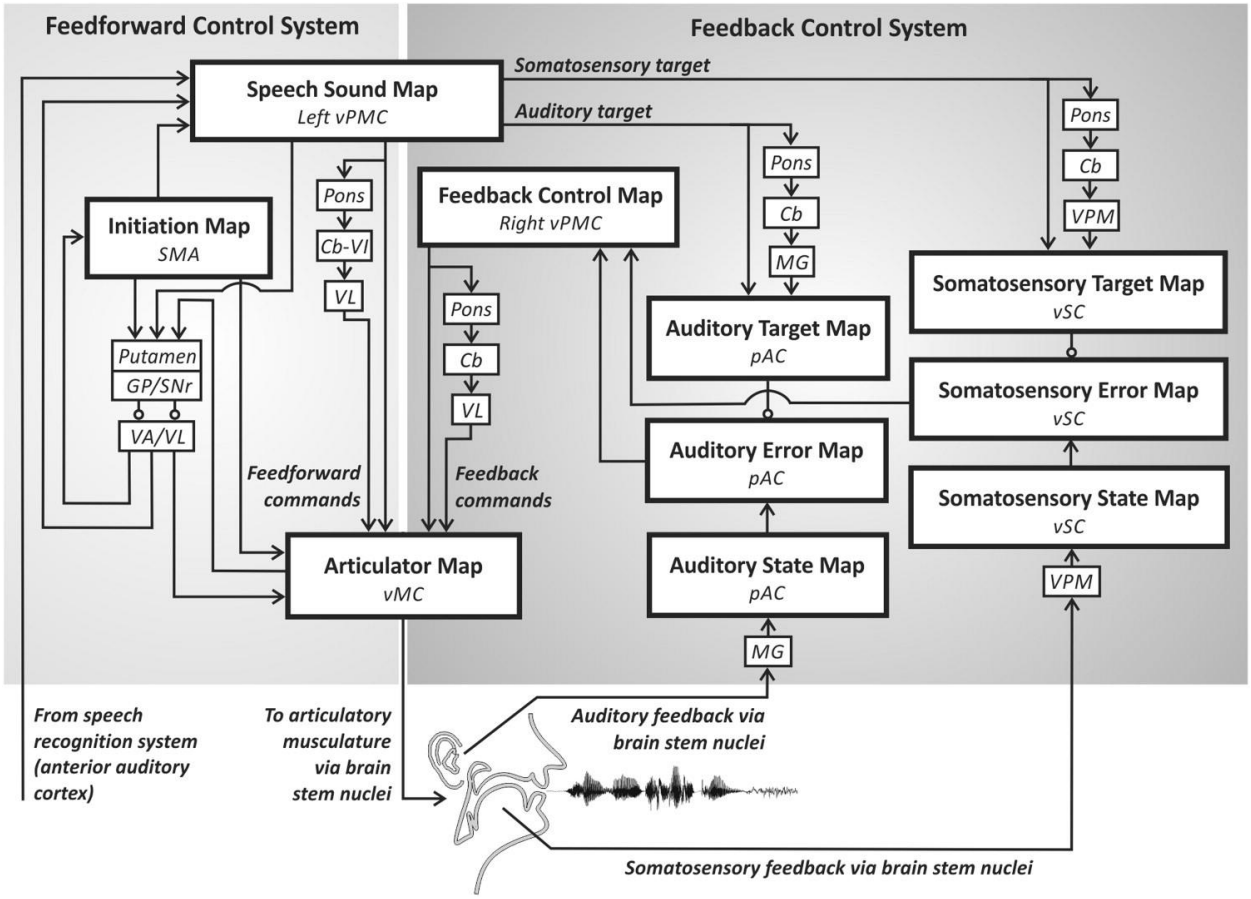

Figure 3: The DIVA model and its neural representations. Boxes indicate nodes (in bold) in the network model with hypothesized representations in specific brain regions (in italics). Abbreviations in order of appearance in the text. vPMC: ventral premotor cortex; GP: globus pallidus; SNr: substantia nigra pars reticula; VA: ventral anterior nucleus of the thalamus; VL: ventral lateral nucleus of the thalamus; SMA: supplementary motor area; vMC: ventral motor cortex; Cb-VI: cerebellum lobule VI; pAC: posterior auditory cortex; vSC: ventral somatosensory cortex; Cb: cerebellum; MG: medial geniculate nucleus of the thalamus; VPM: ventral posterior medial nucleus of the thalamus. *Figure reprinted from Kearney and Guenther (2019) with permission from Taylor and Francis.*

Working in parallel to the actual vocalization, one's own voice is constantly monitored in auditory areas. Likewise, proprioceptive information from the articulatory muscles is analyzed through a thalamic projection in the ventral somatosensory cortex. These two channels are the basis for the feedback system ensuring correct speech production. To this end, the left ventral premotor cortex provides a model of the planned speech output in a modality-specific *Target Map* to each of the two feedback loops. If the system detects an error between planned (*target*) and currently perceived (*state*) speech output, the error feedback is projected to the right ventral premotor cortex. From there, the corrective motor commands are passed on to the ventral motor cortex. Based on the information from these two feedback loops, the motor commands are then adjusted appropriately.

We are genetically equipped with the capacity for acquiring language (Friederici et al. 2017). However, the specific speech sounds that are typical for our mother tongue, have to be learned in early childhood. Infants learn to speak naturally and without being instructed, relying on auditory input to understand, learn, and apply syntactic and phonological rules, as well as semantic relations. Without such auditory input during the sensitive period of language acquisition in the first years of life, however, speech cannot be learned properly (Kral and Sharma 2012). Nevertheless, deaf children can acquire language, when growing up in a signing environment or can otherwise learn to sign early.

2.2.4 Deafness and Sign Language Processing

A widespread misconception about signed languages is that signing people from all over the world share one common sign language. Quite the contrary, sign languages are as diverse as spoken languages, since they have evolved independently from one another in deaf communities all over the world. For instance, British Sign Language and American Sign Language are completely different languages and mutually incomprehensible – unlike their spoken counterparts.[6]

[6] People speaking American English or British English have different accents, though. When we learn a second language, our accent reveals our mother tongue (at least in the beginning). Interestingly, signers also display a foreign accent when they learn a second sign language (Hickok et al. 2001).

What signed and spoken languages have in common, though, are similar linguistic properties such as phonology and morphology, as well as semantic concepts and a complex syntactic structure (Swisher 1988; Lillo-Martin and Gajewski 2014). One example is the use of generic expressions, which was observed in deaf children who were deprived of language input. They developed an own sign language including generic expressions without being able to rely on established linguistic models (Goldin-Meadow et al. 2005).

Spoken language can be transformed to written language word by word, while sign language does not have a written equivalence. Deaf signers additionally have to learn the words and rules of their environment's spoken language for reading, writing and lip reading when communicating with speaking people. The most obvious difference between signed and spoken languages is of course their modality. Spoken language is based on auditory-vocal interactions, while sign language relies on visual-gestural communication.

These commonalities and differences between spoken and signed languages have been investigated for decades. Owing to the invention and on-going improvement of various neurophysiological and neuroimaging techniques, we have gained valuable insight into the mechanisms of spoken and signed languages, especially with regard to the underlying neuroanatomical structures and neurophysiological processes.

These have repeatedly been found to be similar in signed and spoken languages. Functional studies comparing spoken and signed language processing repeatedly revealed activation in language regions also known for spoken language processing (MacSweeney et al. 2002, 2008; Soderfeldt et al. 1994; Emmorey et al. 2003), providing growing evidence for the modality-independence of the language network and the view that sign languages are not merely collections of gestures, but equal to spoken languages in their linguistic nature.

Signed prosody, which is conveyed by facial expression, head and trunk posture, seems to be supported by the same regions in the right hemisphere that are involved in the processing of spoken prosody (Sandler 2012). Besides, signs are accompanied by mouthing, a silent articulation that helps to distinguish similar signs. Therefore, the decoding of sign language in all its complexity requires a fine-grained visuospatial analysis. In addition to the regions also known from spoken language and primary visual areas, sign language

processing involves face perception and biological motion circuits in the right anterior fusiform gyrus and the posterior superior temporal sulcus (Newman et al. 2010).

The specific structural and functional connectivity in the brain of deaf signers can be related to both signing and auditory deprivation. Alterations in the language and speech network that are due to early deafness have previously been addressed functionally and with regard to structural alterations. Several studies have revealed partial takeover of auditory areas in deaf individuals by the visual (Finney et al. 2001; Sharma et al. 2015) and the somatosensory systems (Sharma et al. 2015), while others focused on cortical volume differences (Emmorey et al. 2003; Husain et al. 2011; Li et al. 2012).

In this area, structural magnetic resonance imaging (MRI) has proven to be a well-suited means of studying brain plasticity, being able to capture short-term as well as long-term learning-induced cortical changes in both grey and white matter (Draganski et al. 2004; Schlegel et al. 2012).

2.3 Objective

Regarding functional and structural alterations in the brain that are related to deafness and/or sign language use, two main findings are frequently reported in the literature:

a) White matter changes are found along the hearing pathway and in auditory and language-related cortical regions in deaf individuals.

b) Similar regions are involved in signed and spoken language processing.

These findings raise two hypotheses for investigating the language network in deaf and hearing participants (Finkl et al. 2020):

1. Connectivity changes should be present in the cortical auditory input system of deaf signers. Likewise, articulatory planning connections in the output system should be altered in deaf signers, since they are only used to a basic extent, too.
2. In the core language network, where language as such is processed, connectivity should be comparable between groups.

In order to investigate these hypotheses, language network connectivity of deaf and hearing participants was examined based on the proposition of a language network with a core part for language processing and associated input/output systems for speech processing (Friederici et al. 2017).

2.4 Methodology

2.4.1 Diffusion-weighted magnetic resonance imaging

A widely used method for investigating white matter connectivity is diffusion-weighted magnetic resonance imaging (dMRI). It constitutes the basis for different methods that are used for scientific purposes and is a valuable tool in clinical settings, for example in the diagnosis of multiple sclerosis, dementia, tumors, stroke, and other diseases (Le Bihan et al. 2001). Based on a concept described in the 1960s (Stejskal and Tanner 1965), dMRI has become increasingly popular in neuroscientific research in the 1980s (Le Bihan et al. 1986), owing to its non-invasiveness and its increasing number of possible applications, one of them being tractography. It is currently the state of the art technique for investigating white matter connectivity in the human brain as it allows the reconstruction of fiber tracts based on the diffusion of water molecules in-vivo.

Diffusion is a process that describes the movement of molecules, atoms, particles, and ions along a concentration gradient from high to low without external intervention. The magnetic and diffusion properties of water molecules, together with their omnipresence in the human body, are essential prerequisites for dMRI. Two types of diffusion of water molecules occur in the brain: isotropic and anisotropic diffusion. *Isotropic diffusion* takes place in an environment without obstacles. This can be observed in the ventricles filled with cerebrospinal fluid, where water molecules can move freely in any direction. White matter structure, however, is characterized by fiber bundles consisting of parallel myelinated axons. These pathways in the central nervous system are classified depending on their trajectories. Three main types are differentiated:

1. Association fibers connect cortical regions within the same hemisphere. Short association fibers, also called U-fibers because of their shape, link adjacent gyri or regions like primary and secondary auditory cortices. Long association fibers are crucial for larger functional networks in that they connect cortical regions further apart. For example, the arcuate fasciculus as key tract in the language network connects language-associated regions in the frontal, parietal and temporal lobes.

2. Commissural fibers connect corresponding brain regions of the left and right hemisphere such as left and right auditory cortices.

3. Projection fibers can be ascending or descending. Ascending projections such as the auditory radiation carry information towards the brain, and descending projections, for example from the auditory cortex to auditory nuclei in the brainstem, pass information from the cortex to the brainstem and below.

In this environment of tightly packed fiber bundles, diffusion in the extracellular space becomes *anisotropic*, meaning that water molecules move predominantly along the fiber bundles and less perpendicular to them. In grey matter, cell bodies also pose boundaries to diffusion, but in a less organized way than in white matter. Therefore, diffusivity in grey matter is rather isotropic, but restricted.

For DTI, a three-dimensional diffusion tensor is estimated based on rate and direction of diffusion extracted from at least six diffusion-weighted and one non-diffusion-weighted measurement. It is represented by its three eigenvalues ($\lambda_1, \lambda_2, \lambda_3$) and depicted in the form of an ellipsoid that can take any possible form between a perfect sphere ($\lambda_1 = \lambda_2 = \lambda_3$), a circular plane ($\lambda_1 << \lambda_2 = \lambda_3$) and a straight line ($\lambda_1 >> \lambda_2 = \lambda_3$).

From the diffusion tensor, different parameters can be computed that are often reported in dMRI studies on white matter integrity. *Axial diffusivity* (AD) is a measure for the amount of diffusion along the main direction (λ_1), while *radial diffusivity* (RD) refers to diffusion perpendicular to it (λ_2 and λ_3). *Fractional anisotropy* (FA) is a measure of the directionality of diffusion in a voxel by taking into account the different diffusion directions, thus depending on AD and RD. It can take values from 0 (perfectly isotropic diffusion) to 1 (anisotropic diffusion along a single axis). High FA values indicate dense axonal packing, large axonal diameter and/or high myelination, while low FA values point to axonal degeneration and/or demyelination. *Mean diffusivity* (MD) describes the overall diffusion in a specific voxel independent of directionality, being inversely related to FA values. Strongly organized, thick and/or well-myelinated fiber bundles lead to low MD values, while demyelination and/or axonal degeneration allow for more overall diffusion (Feldman et al.

2010; Alexander et al. 2011). However, these measures should be interpreted with caution, since there is no exact translation to underlying structure.

2.4.2 Deterministic Tractography

By measuring diffusion in the whole brain, the main direction of diffusion in every voxel can be determined. This allows for inferring the trajectory of fibers in the brain and constitutes the basis for tractography (Basser et al. 2000). Deterministic (or streamline) fiber tracking is used to reconstruct streamlines starting from a seed voxel and following the strongest interpolated eigenvectors of voxel after voxel until reaching arbitrary stopping criteria such as low FA (usually below 0.15, indicating the absence of a strong principal direction, as in grey matter) or very sharp curves (to avoid improbable turns and recurring tracts). This works well for voxels covering axons that are part of the same tract and run in parallel, thus leading to strong anisotropic diffusion with one pronounced diffusion direction. However, in the brain, pathways also cross each other at various locations, their axons fan out at the end of the tract or they display sharp curves, all of which can lead to a variety of diffusion directions – and therefore low FA – in a single voxel. These are situations in which deterministic tractography fails. To address this issue, more robust fiber tracking techniques based on a probabilistic approach have evolved that take these factors into account (Behrens et al. 2003).

2.4.3 Probabilistic Tractography

Just as for deterministic fiber tracking, the basis for probabilistic tractography are measures of diffusion, reflected in the diffusion tensor. In deterministic tractography, the streamline follows only the principal direction in each voxel, while probabilistic fiber tracking accounts for other possible trajectories by transforming the diffusion tensor into a fiber orientation tensor. Here, strong directionality indicates a high probability that the fibers are oriented in this direction, while other fiber orientations might be possible, but less likely. To represent these different possible fiber orientations, in probabilistic tractography thousands of paths

are generated from every seed voxel. Every path entering a voxel continues in a certain direction depending on its respective probability.

The more likely a certain fiber orientation is in a voxel, the more paths will follow its trajectory. This iterative procedure results in a three-dimensional map displaying the number of paths that have passed through every voxel, thus representing the connection probability of the seed voxels with every voxel in the map. Probabilistic tracking is usually also stopped at very sharp curves, but not when FA drops, owing to its capacity of modeling the distribution of different possible fiber orientations (Jones 2008).

There is no perfect tractography method and depending on the question investigated, one has to choose carefully which of the many different tracking algorithms to use and how to interpret the results, as both deterministic and probabilistic tractography are only indirect measures of connectivity and have their shortcomings (Maier-Hein et al. 2017). However, major advancements have been made in recent years aiming at improving accuracy and precision of tractography. The most important reasons in favor of choosing probabilistic tractography for this study were the possibility of 1) using complex crossing fiber models that provide better results in regions with low anisotropy due to different possible fiber orientations (Behrens et al. 2007) and 2) comparing the groups' probability maps quantitatively with regard to the different seed regions of interest (ROIs).

2.4.4 Study design and participants

In this work, connectivity of the speech- and language network in ten deaf signers and ten hearing non-signers was analyzed by means of probabilistic tractography. Tracking was started from six seed ROIs in each hemisphere, covering the auditory input system (Heschl's gyrus), the core language network (BA44, posterior superior and posterior middle temporal gyrus, central part of the inferior parietal lobule) and the pre-motor output system (ventral BA6). In addition, two control pathways were tracked from left and right primary visual cortex. The resulting connectivity maps were then compared between groups. For details please see Finkl et al. (2020).

2.5 Results and implications

The deaf group displayed lower connectivity values in the tracts involved in speech perception. The effects were most pronounced in the transcallosal connections between left and right Heschl's gyri, in the continuation of the left-to-right connection towards the contralateral parietal and posterior temporal cortices as well as in the connections of the left Heschl's gyrus towards the ipsilateral parietal cortex. Connection probability was also reduced in tracts subserving speech production, in particular the Broca-Thalamus-preSMA-loop. These results corroborate the first hypothesis pointing at white matter differences between the groups in the input/output parts of the language network. Tracts of the core language network – in particular the SLF/AF and ventral fronto-temporo-parietal connections – had similar connectivity in both groups, supporting the second hypothesis about similar connectivity in the core language network of both groups. For a detailed description of the results please see Finkl et al. (2020).

These findings bear several implications. First, they add another piece of evidence to the modality-independence of the language network in the brain that has been documented in several functional imaging studies (Soderfeldt et al. 1994; MacSweeney et al. 2002, 2008; Emmorey et al. 2003). In addition, the results provide structural groundings for the segregation of language and speech processing (Berwick et al. 2013; Friederici et al. 2017). More specifically, the study shows that prelingual deafness does not affect the classic language pathways, but changes the connectivity of sensory and motor planning areas necessary for the processing of spoken language.

Second, the results stress the potential of sign language use in early childhood for the development of a functioning language network. This becomes particularly important for children with congenital or prelingual deafness who are to be fitted with a cochlear implant (CI). The goal for these children is to reach free understanding of speech and learning to speak. Here, the time point of implantation and therefore the duration of deafness is crucial for a successful outcome after cochlear implantation (Kral and Sharma 2012). For a long time, it was considered counterproductive to sign with these children, as this might diminish their motivation to speak after already having acquired another means of

communication. In contrast, newer studies point to an improved CI outcome with previous sign language acquisition (Campbell et al. 2014).

The present results of a preserved core language network in the deaf group support these findings. In signing children with a CI, the new auditory stimulus conveyed by the CI reaches an established language network and can thus be processed appropriately, while those children who were deprived of any language input before implantation did not have the chance to develop a functioning core language processing network. Therefore, the months or even years before the implantation are crucial for setting the basis for a functioning language network (Twomey et al. 2020) and later speech acquisition with CI – be it developed by speech or sign. Generally, it is beneficial for a successful outcome to implant as early as possible after the diagnosis has been established. The later the implantation occurs, however, the more important language stimulation – of any modality – becomes before.

Third, by adding a piece of evidence to the puzzle of language processing in the brain, this study can contribute to better understanding, diagnostic and treatment of neurological conditions affecting language. In turn, patient studies with individuals suffering from language- and speech-related disorders such as aphasia yield important insights into underlying brain anatomy and function (Wilson et al. 2010).

Last, the results are also relevant from a socio-political perspective. As described earlier, signed and spoken languages display similar linguistic properties (Stokoe 2005). According to the World Federation of the Deaf, however, only 41 of 193 United Nations member countries have legally recognized sign languages (World Federation of the Deaf 2020). Although the legal status of a sign language is not automatically linked to a positive public reception, it is an important act towards more awareness and better opportunities for deaf people. Without this recognition and respective measures taken, it is more difficult for deaf people to develop their cultural and linguistic identity, which can affect their psychological well-being negatively (Chapman and Dammeyer 2017).

In December 2017, the United Nations passed a resolution declaring the International Day of Sign Languages on 23 September "*in order to raise awareness of the importance of sign language in the full realization of the human rights of people who are deaf*" (United

Nations General Assembly 2017, p. 2). This was based on the *Convention on the Rights of Persons with Disabilities* stating „*that sign languages are equal to spoken languages, and that States parties to the Convention undertake to recognize, accept and promote the use of sign languages*“ (United Nations General Assembly 2017, p. 1). Studies like this, showing that signed and spoken languages, in addition to being characterized by similar linguistic properties, also share a common processing network in the brain hopefully contribute to a better understanding, recognition and acceptance of sign languages.

2.6 Outlook

Based on these findings, a number of questions could be addressed. In this study, hearing non-signers were compared with deaf signers, which does not allow conclusive interpretation of the group differences with regard to their cause. In order to separate effects of sign language use from changes caused by auditory deprivation, future research should preferably include a group of hearing signers. To complement the results discussed earlier, tracts relevant for sign language processing could be investigated, shifting the seed ROIs from the auditory-vocal regions to the visual-gestural ones. Investigating the underlying brain network connectivity could provide further interesting insights and help understanding brain structure and function. In order to disentangle developmental effects from the deterioration of pathways caused by long-lasting deafness, the language network connectivity of prelingually deaf adults could be compared to that of adults with long-lasting postlingual deafness.

Another interesting topic would be to investigate a clinical application of dMRI with regard to cochlear implantation. Can tractography results or other dMRI measures of connectivity in the language network be employed as a diagnostic tool for the prediction of successful outcome after CI implantation? Different factors are known to influence CI outcome. The most important one is age of onset of deafness, with general cognitive ability, duration of deafness and CI experience further contributing to a successful outcome. However, there exists no diagnostic test for assessing the neuroanatomical prerequisites with regard to potential CI implantation. The standard diagnostic protocol for CI candidates includes cranial MRI to ensure auditory nerve integrity. Extending it with the dMRI sequence would be feasible and could yield helpful results helping patients and physicians decide whether to implant when in doubt.

The most tempting question, however, would be one related to the brain's plastic capacity: How does the language network of prelingually deaf adults change when presented with speech through a CI? As the implant contains a magnet, CI users are advised to undergo MRI only for medically required purposes in order to avoid unnecessary and often painful complications such as displacement of the magnet, which requires surgical

intervention for magnet reposition or exchange (Leinung et al. 2020). In order to circumvent this problem, rotatable magnets have been introduced. However, the metallic parts of the CI cause an artifact in exactly those temporo-parietal regions that are of interest for this research question, an issue that has not been solved to date, leaving the question still unanswered.

Studies comparing signing, speaking, deaf and hearing participants in different combinations have added valuable insight to our understanding of language processing. They have provided evidence for a general similarity concerning core language functions in signed and spoken languages and supported the acceptance of signed languages worldwide. In addition, work on different language systems such as Chinese and German support the idea of a common neural basis for language processing, with variations shaped by the specific linguistic characteristics of a language (Zhang et al. 2017). On this ground, future research focusing on the uniqueness and subtle particularities of different languages could include signed languages to a greater extent, offering insights beyond language processing, as "*the language that we use to communicate acts as a subtle filter through which we understand and interact with the world*" (Evans et al. 2019, p. 3747).

Integrating the quotations from René Descartes and Andrea Moro, we get:

I speak, therefore I think.

(which is logically invalid, but hopefully still true most of the time)

Language is indeed a playground.

2.7 Declaration of contributions

Recruitment of participants

I was responsible for the recruitment of the hearing participants and assisted with the recruitment of the deaf participants.

Data acquisition

DTI data were acquired by radiographers at the University Hospital Dresden. I was present during data acquisition, informed participants about study protocols and data security and filled out the questionnaires and informed consent with them. I also prepared a version in plain language for the deaf participants.

Data analysis

After having been introduced to DTI data analysis, I conducted all steps of data analysis independently: pre-processing, ROI definition, probabilistic tractography and statistical analyses. I improved the method for ROI definition and applied it in this work.

Text

I have written this dissertation without any help from others. I have cited all quotations and paraphrases as well as information from other sources and I have provided the corresponding references.

Figures

I included figures from other sources that I cited with their according references. I have been granted permission by the publishers to use the following figures in this thesis:

- Figure 1: Simplified scheme of the ascending auditory pathways with the most important relay stations and their connections (page 13)
- Figure 2: Schematic and simplified view of the core language network (page 16)
- Figure 3: The DIVA model and its neural representations (page 19)

Tables

I modified Table 1 (page 9) from another source that I cited with the according reference.

Publication

I wrote the manuscript for the publication „Language Without Speech: Segregating Distinct Circuits in the Human Brain“ and considered remarks and suggestions from the co-authors during the submission and revision process. I created all figures and tables in the article and the supplementary material. I was responsible for the correspondence during the publication process, and wrote the cover and response letters.

2.8 References

Alexander AL, Hurley SA, Samsonov AA, Adluru N, Hosseinbor AP, Mossahebi P, Tromp DPM, Zakszewski E, Field AS. 2011. Characterization of Cerebral White Matter Properties Using Quantitative Magnetic Resonance Imaging Stains. Brain Connect. 1:423–446.

Anwander A, Tittgemeyer M, Cramon D von, Friederici AD, Knösche TR. 2007. Connectivity-Based Parcellation of Broca's Area. Cereb Cortex. 17:816–825.

Basser PJ, Pajevic S, Pierpaoli C, Duda J, Aldroubi A. 2000. In vivo fiber tractography using DT-MRI data. Magn Reson Med. 44:625–632.

Behrens TEJ, Berg HJ, Jbabdi S, Rushworth MFS, Woolrich MW. 2007. Probabilistic diffusion tractography with multiple fibre orientations: What can we gain? NeuroImage. 34:144–155.

Behrens TEJ, Woolrich MW, Jenkinson M, Johansen-Berg H, Nunes RG, Clare S, Matthews PM, Brady JM, Smith SM. 2003. Characterization and propagation of uncertainty in diffusion-weighted MR imaging. Magn Reson Med. 50:1077–1088.

Berwick RC, Friederici AD, Chomsky N, Bolhuis JJ. 2013. Evolution, brain, and the nature of language. Trends Cogn Sci. 17:89–98.

Campbell R, MacSweeney M, Woll B. 2014. Cochlear implantation (CI) for prelingual deafness: the relevance of studies of brain organization and the role of first language acquisition in considering outcome success. Front Hum Neurosci. 8.

Chapman M, Dammeyer J. 2017. The Significance of Deaf Identity for Psychological Well-Being. J Deaf Stud Deaf Educ. 22:187–194.

D'Esposito M, Postle BR. 2015. The cognitive neuroscience of working memory. Annu Rev Psychol. 66:115–142.

Draganski B, Gaser C, Busch V, Schuierer G, Bogdahn U, May A. 2004. Neuroplasticity: Changes in grey matter induced by training. Nature. 427:311–312.

Emmorey K, Allen JS, Bruss J, Schenker N, Damasio H. 2003. A morphometric analysis of auditory brain regions in congenitally deaf adults. Proc Natl Acad Sci. 100:10049–10054.

Emmorey K, Grabowski T, McCullough S, Damasio H, Ponto LLB, Hichwa RD, Bellugi U. 2003. Neural systems underlying lexical retrieval for sign language. Neuropsychologia. 41:85–95.

Evans S, Price CJ, Diedrichsen J, Gutierrez-Sigut E, MacSweeney M. 2019. Sign and Speech Share Partially Overlapping Conceptual Representations. Curr Biol. 29:3739-3747.e5.

Feldman HM, Yeatman JD, Lee ES, Barde LHF, Gaman-Bean S. 2010. Diffusion Tensor Imaging: A Review for Pediatric Researchers and Clinicians. J Dev Behav Pediatr. 31:346–356.

Finkl T, Hahne A, Friederici AD, Gerber J, Mürbe D, Anwander A. 2020. Language Without Speech: Segregating Distinct Circuits in the Human Brain. Cereb Cortex. 30:812–823.

Finney EM, Fine I, Dobkins KR. 2001. Visual stimuli activate auditory cortex in the deaf. Nat Neurosci. 4:1171–1173.

Fitch WT, Hauser MD. 2004. Computational Constraints on Syntactic Processing in a Nonhuman Primate. Science. 303:377–380.

Friederici AD. 2011. The Brain Basis of Language Processing: From Structure to Function. Physiol Rev. 91:1357–1392.

Friederici AD. 2017. Language in our brain: the origins of a uniquely human capacity. Cambridge (MA): The MIT Press.

Friederici AD, Chomsky N, Berwick RC, Moro A, Bolhuis JJ. 2017. Language, mind and brain. Nat Hum Behav. 1:713–722.

Friederici AD, Meyer M, von Cramon DY. 2000. Auditory Language Comprehension: An Event-Related fMRI Study on the Processing of Syntactic and Lexical Information. Brain Lang. 74:289–300.

Geschwind N. 1970. The Organization of Language and the Brain: Language disorders after brain damage help in elucidating the neural basis of verbal behavior. Science. 170:940–944.

Goldin-Meadow S, Gelman SA, Mylander C. 2005. Expressing generic concepts with and without a language model. Cognition. 96:109–126.

Guenther FH. 1995. Speech sound acquisition, coarticulation, and rate effects in a neural network model of speech production. Psychol Rev. 102:594–621.

Hackett TA. 2015. Chapter 2 - Anatomic organization of the auditory cortex. In: Aminoff MJ, Boller F, Swaab DF, editors. Handbook of Clinical Neurology. The Human Auditory System. Amsterdam (Netherlands): Elsevier. p. 27–53.

Häkkinen S, Rinne T. 2018. Intrinsic, stimulus-driven and task-dependent connectivity in human auditory cortex. Brain Struct Funct. 223:2113–2127.

Hickok G, Bellugi U, Klima ES. 2001. Sign language in the brain. Sci Am. 284:58–65.

Hickok G, Poeppel D. 2007. The cortical organization of speech processing. Nat Rev Neurosci. 8:393–402.

Husain FT, Medina RE, Davis CW, Szymko-Bennett Y, Simonyan K, Pajor NM, Horwitz B. 2011. Neuroanatomical changes due to hearing loss and chronic tinnitus: A combined VBM and DTI study. Brain Res. 1369:74–88.

Jones DK. 2008. Studying connections in the living human brain with diffusion MRI. Cortex, Special Issue on “Brain Hodology - Revisiting disconnection approaches to disorders of cognitive function.” 44:936–952.

Kearney E, Guenther FH. 2019. Articulating: the neural mechanisms of speech production. Lang Cogn Neurosci. 34:1214–1229.

Kral A, Sharma A. 2012. Developmental neuroplasticity after cochlear implantation. Trends Neurosci. 35:111–122.

Le Bihan D, Breton E, Lallemand D, Grenier P, Cabanis E, Laval-Jeantet M. 1986. MR imaging of intravoxel incoherent motions: application to diffusion and perfusion in neurologic disorders. Radiology. 161:401–407.

Le Bihan D, Mangin J-F, Poupon C, Clark CA, Pappata S, Molko N, Chabriat H. 2001. Diffusion tensor imaging: Concepts and applications. J Magn Reson Imaging. 13:534–546.

Leinung M, Loth A, Gröger M, Burck I, Vogl T, Stöver T, Helbig S. 2020. Cochlear implant magnet dislocation after MRI: surgical management and outcome. Eur Arch Otorhinolaryngol. 277:1297–1304.

Li Y, Ding G, Booth JR, Huang R, Lv Y, Zang Y, He Y, Peng D. 2012. Sensitive period for white-matter connectivity of superior temporal cortex in deaf people. Hum Brain Mapp. 33:349–359.

Lillo-Martin DC, Gajewski J. 2014. One grammar or two? Sign Languages and the Nature of Human Language. WIREs Cogn Sci. 5:387–401.

MacSweeney M, Capek CM, Campbell R, Woll B. 2008. The signing brain: the neurobiology of sign language. Trends Cogn Sci. 12:432–440.

MacSweeney M, Woll B, Campbell R, McGuire PK, David AS, Williams SCR, Suckling J, Calvert GA, Brammer MJ. 2002. Neural systems underlying British Sign Language and audio-visual English processing in native users. Brain. 125:1583–1593.

Maier-Hein KH, Neher PF, Houde J-C, Côté M-A, Garyfallidis E, Zhong J, Chamberland M, Yeh F-C, Lin Y-C, Ji Q, Reddick WE, Glass JO, Chen DQ, Feng Y, Gao C, Wu Y, Ma J, He R, Li Q, Westin C-F, Deslauriers-Gauthier S, González JOO, Paquette M, St-Jean S, Girard G, Rheault F, Sidhu J, Tax CMW, Guo F, Mesri HY, Dávid S, Froeling M, Heemskerk AM,

Leemans A, Boré A, Pinsard B, Bedetti C, Desrosiers M, Brambati S, Doyon J, Sarica A, Vasta R, Cerasa A, Quattrone A, Yeatman J, Khan AR, Hodges W, Alexander S, Romascano D, Barakovic M, Auría A, Esteban O, Lemkaddem A, Thiran J-P, Cetingul HE, Odry BL, Mailhe B, Nadar MS, Pizzagalli F, Prasad G, Villalon-Reina JE, Galvis J, Thompson PM, Requejo FDS, Laguna PL, Lacerda LM, Barrett R, Dell'Acqua F, Catani M, Petit L, Caruyer E, Daducci A, Dyrby TB, Holland-Letz T, Hilgetag CC, Stieltjes B, Descoteaux M. 2017. The challenge of mapping the human connectome based on diffusion tractography. Nat Commun. 8:1–13.

Mazoyer B, Zago L, Jobard G, Crivello F, Joliot M, Perchey G, Mellet E, Petit L, Tzourio-Mazoyer N. 2014. Gaussian Mixture Modeling of Hemispheric Lateralization for Language in a Large Sample of Healthy Individuals Balanced for Handedness. PLOS ONE. 9:e101165.

Meyer J. 2008. Typology and acoustic strategies of whistled languages: Phonetic comparison and perceptual cues of whistled vowels. J Int Phon Assoc. 38:69–94.

Meyer L, Obleser J, Friederici AD. 2013. Left parietal alpha enhancement during working memory-intensive sentence processing. Cortex. 49:711–721.

Newman AJ, Supalla T, Hauser PC, Newport EL, Bavelier D. 2010. Prosodic and narrative processing in American Sign Language: An fMRI study. NeuroImage. 52:669–676.

Perani D, Saccuman MC, Scifo P, Anwander A, Spada D, Baldoli C, Poloniato A, Lohmann G, Friederici AD. 2011. Neural language networks at birth. Proc Natl Acad Sci U S A. 108:16056–16061.

Pickles JO. 2013. An introduction to the physiology of hearing. 4th ed. Leiden: Brill.

Pickles JO. 2015. Chapter 1 - Auditory pathways: anatomy and physiology. In: Aminoff MJ, Boller F, Swaab DF, editors. Handbook of Clinical Neurology. The Human Auditory System. Amsterdam (Netherlands): Elsevier. p. 3–25.

Rilling JK, Glasser MF, Preuss TM, Ma X, Zhao T, Hu X, Behrens TEJ. 2008. The evolution of the arcuate fasciculus revealed with comparative DTI. Nat Neurosci. 11:426–428.

Sammler D, Grosbras M-H, Anwander A, Bestelmeyer PEG, Belin P. 2015. Dorsal and Ventral Pathways for Prosody. Curr Biol. 25:3079–3085.

Sandler W. 2012. The Phonological Organization of Sign Languages. Lang Linguist Compass. 6:162–182.

Schlegel AA, Rudelson JJ, Tse PU. 2012. White Matter Structure Changes as Adults Learn a Second Language. J Cogn Neurosci. 24:1664–1670.

Seydell-Greenwald A, Chambers CE, Ferrara K, Newport EL. 2020. What you say versus how you say it: Comparing sentence comprehension and emotional prosody processing using fMRI. NeuroImage. 209:116509.

Sharma A, Campbell J, Cardon G. 2015. Developmental and cross-modal plasticity in deafness: Evidence from the P1 and N1 event related potentials in cochlear implanted children. Int J Psychophysiol, Recent advances in auditory perception. 95:135–144.

Shearer AE, Hildebrand MS, Smith RJ. 1993. Hereditary Hearing Loss and Deafness Overview. In: Adam MP, Ardinger HH, Pagon RA, Wallace SE, Bean LJ, Stephens K, Amemiya A, editors. GeneReviews®. Seattle (WA): University of Washington, Seattle.

Sheffield AM, Smith RJH. 2019. The Epidemiology of Deafness. Cold Spring Harb Perspect Med. 9:a033258.

Slevc LR, Shell AR. 2015. Chapter 32 - Auditory agnosia. In: Aminoff MJ, Boller F, Swaab DF, editors. Handbook of Clinical Neurology. The Human Auditory System. Amsterdam (Netherlands): Elsevier. p. 573–587.

Soderfeldt B, Ronnberg J, Risberg J. 1994. Regional Cerebral Blood Flow in Sign Language Users. Brain Lang. 46:59–68.

Spormann-Lagodzinski ME, Nubel K, König O, Gross M. 2003. Ätiologie und Prävalenz permanenter kindlicher Hörstörungen in Deutschland. In: Aktuelle phoniatrisch-pädaudiologische Aspekte. Presented at the 20. Wissenschaftliche Jahrestagung der DGPP. Ger Med Sci. p. DocV37.

Stejskal EO, Tanner JE. 1965. Spin Diffusion Measurements: Spin Echoes in the Presence of a Time-Dependent Field Gradient. J Chem Phys. 42:288–292.

Stokoe WC. 2005. Sign Language Structure: An Outline of the Visual Communication Systems of the American Deaf. J Deaf Stud Deaf Educ. 10:3–37.

Swisher VM. 1988. Similarities and Differences between Spoken Languages and Natural Sign Languages. Appl Linguist. 9:343–356.

Telkemeyer S, Rossi S, Koch SP, Nierhaus T, Steinbrink J, Poeppel D, Obrig H, Wartenburger I. 2009. Sensitivity of Newborn Auditory Cortex to the Temporal Structure of Sounds. J Neurosci. 29:14726–14733.

Twomey T, Price CJ, Waters D, MacSweeney M. 2020. The impact of early language exposure on the neural system supporting language in deaf and hearing adults. NeuroImage. 209:116411.

Ungerleider LG, Mishkin M. 1982. Two Cortical Visual Systems. In: Ingle DJ, Goodale MA, Mansfield RJW, editors. Analysis of visual behavior. Cambridge (MA): The MIT Press. p. 549–586.

United Nations General Assembly. 2017. International Day of Sign Languages (Resolution No. 72/161). United Nations General Assembly.

von Gablenz P, Hoffmann E, Holube I. 2017. Prävalenz von Schwerhörigkeit in Nord- und Süddeutschland. HNO. 65:663–670.

Weichbold V, Nekahm-Heis D, Welzl-Müller K. 2005. Zehn Jahre Neugeborenen-Hörscreening in Österreich: Eine Evaluierung. Wien Klin Wochenschr. 117:641–646.

Wilson SM, Dronkers NF, Ogar JM, Jang J, Growdon ME, Agosta F, Henry ML, Miller BL, Gorno-Tempini ML. 2010. Neural Correlates of Syntactic Processing in the Nonfluent Variant of Primary Progressive Aphasia. J Neurosci. 30:16845–16854.

World Federation of the Deaf. 2020. WFD | The Legal Recognition of Sign Languages by Country [WWW Document]. WFD. URL https://wfdeaf.org/news/resources/legal-recognition-sign-languages-country/. Accessed February 2nd, 2020.

World Health Organization. 2020. WHO | Grades of hearing impairment [WWW Document]. WHO. URL http://www.who.int/deafness/hearing_impairment_grades/en/. Accessed May 2nd, 2020.

Zatorre RJ, Mondor TA, Evans AC. 1999. Auditory Attention to Space and Frequency Activates Similar Cerebral Systems. NeuroImage. 10:544–554.

Zhang Y, Fan L, Caspers S, Heim S, Song M, Liu C, Mo Y, Eickhoff SB, Amunts K, Jiang T. 2017. Cross-cultural consistency and diversity in intrinsic functional organization of Broca's Region. NeuroImage. 150:177–190.

3 EIDESSTATTLICHE VERSICHERUNG UND ANTEILSERKLÄRUNG

3.1 Eidesstattliche Versicherung

„Ich, Theresa Finkl, versichere an Eides statt durch meine eigenhändige Unterschrift, dass ich die vorgelegte Dissertation mit dem Thema: „Probabilistic tractography of the neural language network in deaf and hearing adults // Probabilistische Traktographie des neuronalen Sprachnetzwerks bei tauben und hörenden Erwachsenen“, selbstständig und ohne nicht offengelegte Hilfe Dritter verfasst und keine anderen als die angegebenen Quellen und Hilfsmittel genutzt habe.

Alle Stellen, die wörtlich oder dem Sinne nach auf Publikationen oder Vorträgen anderer Autoren beruhen, sind als solche in korrekter Zitierung kenntlich gemacht. Die Abschnitte zu Methodik (insbesondere praktische Arbeiten, Laborbestimmungen, statistische Aufarbeitung) und Resultaten (insbesondere Abbildungen, Graphiken und Tabellen) werden von mir verantwortet.

Meine Anteile an etwaigen Publikationen zu dieser Dissertation entsprechen denen, die in der untenstehenden gemeinsamen Erklärung mit dem Erstbetreuer angegeben sind. Für sämtliche im Rahmen der Dissertation entstandenen Publikationen wurden die Richtlinien des ICMJE (International Committee of Medical Journal Editors; http://www.icmje.org) zur Autorenschaft eingehalten. Ich erkläre ferner, dass mir die Satzung der Charité – Universitätsmedizin Berlin zur Sicherung Guter Wissenschaftlicher Praxis bekannt ist und ich mich zur Einhaltung dieser Satzung verpflichte.

Die Bedeutung dieser eidesstattlichen Versicherung und die strafrechtlichen Folgen einer unwahren eidesstattlichen Versicherung (§§156, 161 des Strafgesetzbuches) sind mir bekannt und bewusst.“

_____	_____
Datum	Unterschrift der Doktorandin

3.2 Anteilserklärung an der erfolgten Publikation

Theresa Finkl, Anja Hahne, Angela D Friederici, Johannes Gerber, Dirk Mürbe, Alfred Anwander, **Language Without Speech: Segregating Distinct Circuits in the Human Brain**, *Cerebral Cortex*, Volume 30, Issue 2, February 2020, Pages 812–823, https://doi.org/10.1093/cercor/bhz128, *online publiziert im August 2019*

Rekrutierung der Proband*innen

Ich war zuständig für die Rekrutierung der hörenden Teilnehmenden und habe bei der Rekrutierung der tauben Teilnehmenden mitgewirkt.

Datenerhebung

Die DTI-Daten wurden von den medizinisch-technischen Radiologieassistent*innen des Universitätsklinikums Dresden erhoben. Ich war bei den Messungen anwesend und habe die Proband*innen über Studie, Datenschutz und geplantes Vorgehen aufgeklärt sowie zusammen mit ihnen die Fragebögen zu ihren demographischen Daten und die Einverständniserklärung zur Studie bearbeitet, welche ich selbst erstellt habe. Für die tauben Teilnehmenden formulierte ich jeweils auch eine Version in einfacher Sprache.

Datenanalyse

Ich wurde von Alfred Anwander in die DTI-Analysen eingearbeitet und während des Auswerteprozesses in allen Fragen unterstützt. Die Vorverarbeitung der Daten sowie die ROI Definition und die Traktographie habe ich selbstständig durchgeführt, ebenso alle statistischen Tests.

Schreiben der Publikation

Ich bin alleinige Erstautorin der Publikation und habe das gesamte Manuskript geschrieben. Dabei habe ich vor der Einreichung und in den Revisionsschleifen die Anmerkungen der Co-Autoren berücksichtigt und eingearbeitet.

Grafiken und Tabellen

Ich habe alle Grafiken und Tabellen im Artikel und im Supplement selbst erstellt.

Korrespondenz

Ich habe die Korrespondenz während des Publikationsprozesses verantwortet und durchgeführt. Alfred Anwander und Anja Hahne sind ebenfalls als Kontaktpersonen angegeben, da zum Zeitpunkt der Einreichung bereits absehbar war, dass ich die TU Dresden verlassen würde. Ich hatte deshalb mit den beiden vereinbart, dass sie mir eventuelle Anfragen nach der Veröffentlichung weiterleiten.

_____ _____

Datum Unterschrift der Doktorandin

4 AUSZUG AUS DER JOURNAL SUMMARY LIST

Journal Data Filtered By: **Selected JCR Year: 2017** Selected Editions: SCIE,SSCI
Selected Categories: **"NEUROSCIENCES"** Selected Category Scheme: WoS
Gesamtanzahl: 261 Journale

Rank	Full Journal Title	Total Cites	Journal Impact Factor	Eigenfactor Score
1	NATURE REVIEWS NEUROSCIENCE	40,834	32.635	0.069940
2	NATURE NEUROSCIENCE	59,426	19.912	0.153710
3	ACTA NEUROPATHOLOGICA	18,783	15.872	0.041490
4	TRENDS IN COGNITIVE SCIENCES	25,391	15.557	0.040790
5	BEHAVIORAL AND BRAIN SCIENCES	8,900	15.071	0.010130
6	Annual Review of Neuroscience	13,320	14.675	0.016110
7	NEURON	89,410	14.318	0.216730
8	PROGRESS IN NEUROBIOLOGY	13,065	14.163	0.015550
9	BIOLOGICAL PSYCHIATRY	42,494	11.982	0.056910
10	MOLECULAR PSYCHIATRY	18,460	11.640	0.047200
11	JOURNAL OF PINEAL RESEARCH	9,079	11.613	0.008600
12	TRENDS IN NEUROSCIENCES	20,061	11.439	0.026860
13	BRAIN	52,061	10.840	0.075170
14	SLEEP MEDICINE REVIEWS	6,080	10.602	0.010720
15	ANNALS OF NEUROLOGY	37,251	10.244	0.053390
16	Translational Stroke Research	2,202	8.266	0.005260
17	NEUROSCIENCE AND BIOBEHAVIORAL REVIEWS	24,279	8.037	0.048460
18	NEUROSCIENTIST	4,738	7.461	0.008730
19	NEURAL NETWORKS	10,086	7.197	0.015290
20	FRONTIERS IN NEUROENDOCRINOLOGY	3,924	6.875	0.006040
21	NEUROPSYCHOPHARMACOLOGY	24,537	6.544	0.042870
22	CURRENT OPINION IN NEUROBIOLOGY	14,190	6.541	0.034670
23	Molecular Neurodegeneration	3,489	6.426	0.009850
24	CEREBRAL CORTEX	29,570	6.308	0.058970
25	BRAIN BEHAVIOR AND IMMUNITY	12,583	6.306	0.026850
26	BRAIN PATHOLOGY	4,952	6.187	0.007750
27	Brain Stimulation	4,263	6.120	0.014510
28	NEUROPATHOLOGY AND APPLIED NEUROBIOLOGY	3,654	6.059	0.006350
29	JOURNAL OF CEREBRAL BLOOD FLOW AND METABOLISM	19,450	6.045	0.028280
30	JOURNAL OF NEUROSCIENCE	176,157	5.970	0.265950
31	Molecular Autism	1,679	5.872	0.006320
31	Translational Neurodegeneration	589	5.872	0.002280
33	GLIA	13,417	5.846	0.020530
34	Neurotherapeutics	3,973	5.719	0.008980
35	PAIN	36,132	5.559	0.038000
36	NEUROIMAGE	92,719	5.426	0.152610
37	Acta Neuropathologica Communications	2,326	5.414	0.011550
38	Multiple Sclerosis Journal	10,675	5.280	0.021890

5 DRUCKEXEMPLAR DER PUBLIKATION

5.1 Artikel

Theresa Finkl, Anja Hahne, Angela D Friederici, Johannes Gerber, Dirk Mürbe, Alfred Anwander, **Language Without Speech: Segregating Distinct Circuits in the Human Brain**, *Cerebral Cortex*, Volume 30, Issue 2, February 2020, Pages 812–823, https://doi.org/10.1093/cercor/bhz128, *online publiziert im August 2019*

Cerebral Cortex, February 2020;30: 812–823

doi: 10.1093/cercor/bhz128
Advance Access Publication Date: 2 August 2019
Original Article

Downloaded from https://academic.oup.com/cercor/article-abstract/30/2/812/5543064 by Charité - Med. Bibliothek user on 12 April 2020

ORIGINAL ARTICLE

Language Without Speech: Segregating Distinct Circuits in the Human Brain

Theresa Finkl[1,*], Anja Hahne[1,*], Angela D. Friederici[2], Johannes Gerber[3], Dirk Mürbe[4] and Alfred Anwander[2,*]

[1]Saxonian Cochlear Implant Centre, Phoniatrics and Audiology, Faculty of Medicine, Technische Universität Dresden, Fetscherstraße 74, 01307 Dresden, Germany, [2]Department of Neuropsychology, Max Planck Institute for Human Cognitive and Brain Sciences, 04103 Leipzig, Germany, [3]Neuroradiology, Faculty of Medicine, Technische Universität Dresden, 01304 Dresden, Germany and [4]Department of Audiology and Phoniatrics, Charité—Universitätsmedizin, 10117 Berlin, Germany

Address correspondence to Theresa Finkl/Anja Hahne, Saxonian Cochlear Implant Centre, Phoniatrics and Audiology, Faculty of Medicine, Technische Universität Dresden, Fetscherstraße 74, 01307 Dresden, Germany. Phone: +49 351 458 7048, Email: anja.hahne@ukdd.de or Alfred Anwander, Max Planck Institute for Human Cognitive and Brain Sciences, Stephanstr. 1a, 04103 Leipzig, Germany. Phone: +49 341 9940-2626, Email: anwander@cbs.mpg.de
https://orcid.org/0000-0002-6495-858X https://orcid.org/0000-0002-4861-4808

Abstract

Language is a fundamental part of human cognition. The question of whether language is processed independently of speech, however, is still heavily discussed. The absence of speech in deaf signers offers the opportunity to disentangle language from speech in the human brain. Using probabilistic tractography, we compared brain structural connectivity of adult deaf signers who had learned sign language early in life to that of matched hearing controls. Quantitative comparison of the connectivity profiles revealed that the core language tracts did not differ between signers and controls, confirming that language is independent of speech. In contrast, pathways involved in the production and perception of speech displayed lower connectivity in deaf signers compared to hearing controls. These differences were located in tracts towards the left pre-supplementary motor area and the thalamus when seeding in Broca's area, and in ipsilateral parietal areas and the precuneus with seeds in left posterior temporal regions. Furthermore, the interhemispheric connectivity between the auditory cortices was lower in the deaf than in the hearing group, underlining the importance of the transcallosal connection for early auditory processes. The present results provide evidence for a functional segregation of the neural pathways for language and speech.

Key words: deaf, dMRI, DTI, language network, probabilistic tractography

Introduction

Language is a crucial part of human cognition and communication. The comprehension and production of spoken language requires the interplay between the core language network and the auditory input and motor output systems. Language itself, however, can be acquired independent of modality. This is the case in prelingually deaf individuals, who are either born deaf or lose their hearing before the acquisition of language (Smith et al. 1993). With vision-based sign language as their native language input, they develop language comparable to those of hearing people (Lillo-Martin and Gajewski 2014). Learning to read and write in later childhood consolidates language performance,

© The Author(s) 2019. Published by Oxford University Press.
This is an Open Access article distributed under the terms of the Creative Commons Attribution License (http://creativecommons.org/licenses/by/4.0/), which permits unrestricted reuse, distribution, and reproduction in any medium, provided the original work is properly cited.

though often at a lower level than in hearing non-signers. With additional training prelingually deaf people can also learn to visually decode spoken language primarily via lip reading, and to produce speech, but with clear limitations in the domains of phonation and articulation (Harris and Beech 1998). The unique situation of language without speech in deaf signers offers the possibility to disentangle the neural underpinnings of speech as an input–output system from those of the core language system. In the present study we achieved this by comparing the effect of auditory (oral) and visual (sign) language acquisition on the differential neuroplastic development of the respective structural brain networks.

The exact functional division of language and speech networks continues to be the subject of sustained scientific research. On a theoretical level (Berwick et al. 2013; Friederici et al. 2017), a core language system responsible for semantic and syntactic processes is distinguished from a sensory–motor interface system allowing communication via vocal production and auditory perception of speech. In sign language, this is achieved through the visual decoding of manual gestures and concomitant lip reading. At the neural network level, Broca's area in the left inferior frontal gyrus (IFG) and Wernicke's area in the left posterior temporal cortex extending to the inferior parietal lobule (IPL) are widely accepted as major nodes of the core language network (Price 2012; Hagoort, 2014). This core language network also supports semantic and syntactic processes in sign language (Emmorey et al. 2003; MacSweeney et al. 2002).

The frontal cortex and the temporal cortex also include brain areas relevant for speech production (ventral BA6 in the motor cortex) and for speech perception (Heschl's gyrus (HG) in the auditory cortex). These frontal and posterior temporal brain areas are connected by long-range white matter fiber tracts located dorsally and ventrally to the Sylvian fissure. We will discuss these in turn.

Dorsally, there are two distinguishable fiber pathways. The superior longitudinal/arcuate fasciculus (SLF/AF) connects the posterior portion of Broca's area (BA44) to posterior superior and middle temporal gyri (pSTG and pMTG) touching the IPL on its way (Catani et al. 2005; Anwander et al. 2007; Perani et al. 2011). This fiber tract has been demonstrated to be involved in the development and processing of complex syntactic structures (Friederici et al. 2006; Brauer et al. 2011; Skeide et al. 2016). Another part of the dorsal pathway running in parallel and also involving the SLF/AF targets the ventral precentral gyrus (ventral part of BA6: vBA6) and links speech motor areas to the auditory cortex (Catani et al. 2005; Perani et al. 2011). In a purely functional model Hickok and Poeppel (2007) proposed the dorsal processing stream to support sensory-motor processes, without however, further separating the dorsal stream into substreams. The presently available evidence suggests that there are two dorsal white matter fiber tracts and that the sensory-motor function should be related to the pathway targeting vBA6 (Saur et al. 2008). In an intracranial recording study, it has been shown that BA44 is activated prior to vBA6 during speech production, supporting the view that vBA6 is involved in the articulation of speech following the planning and initiation phase subserved by BA44 (Flinker et al. 2015). These two functionally distinct regions also exhibit differential functional connectivities: the ventral part of BA44 displays connections with language-relevant areas in the temporal and parietal cortex, while vBA6 is linked to input/output-related areas such as the pSTG and the face area in the central and postcentral gyrus responsible for tongue and lip movements (Zhang et al. 2017).

Another fiber tract involved in speaking is the frontal aslant tract (FAT). It connects vBA6 and BA44 as the most posterior parts of what is sometimes called "Broca's territory" (extending from BA44 frontally to BA45 and BA47) with the pre-supplementary motor area (preSMA) and SMA (Catani et al. 2013). This connection is essential for the articulation of words and forms part of the loop between frontal regions such as vBA6 and BA44, the basal ganglia, and the thalamus (Tha; for a review see Dick et al. 2019). It is important to note the FAT's differentiation between vBA6 and BA44 as well as between preSMA and SMA. Together with the cerebellum, these pathways convey information for the finely-tuned activity of the articulatory muscles necessary to produce comprehensible speech, which also implies their participation in the auditory feedback loop during speaking (Petacchi et al. 2005). Little is known about the neural basis for production of facial expressions during sign language production, although mouthing plays a crucial role. In German Sign Language (GSL), for example, the words "brother" and "sister" are performed with the same manual gesture, but different lip patterns. This makes it likely that pathways to vBA6 known to be relevant for speaking may also be relevant for signing.

Ventral to the Sylvian fissure, there are two main fiber tracts connecting the ventral part of the anterior portion of the IFG to the temporal cortex: the uncinate fasciculus and the inferior fronto-occipital fasciculus. Additionally, the inferior longitudinal and the middle longitudinal fasciculus extend posteriorly from the temporal pole. Functionally, these fiber tracts are attributed mainly to the processing of semantic information, but they have also been described in studies on emotion and cognitive control (for a review see Bajada et al. 2015). Among these, the most relevant tract for language processing is the inferior fronto-occipital fasciculus, which has been described to support semantic processes (Saur et al. 2008).

While semantic and syntactic processes are mainly subserved by this left-dominant network, there is increasing evidence that prosodic features of spoken language are processed in a right-dominant network (Sammler et al. 2015; Sammler et al. 2018). The interplay between the left and the right hemisphere during auditory language processing has been demonstrated in patients with lesions in the corpus callosum (CC; Friederici et al. 2007). This hemispheric dissociation between a system for semantic and syntactic processing in the left hemisphere and a system for processing prosodic information in the right hemisphere has also been discovered in sign language, where semantic and syntactic tasks activate the typical left-lateralized language regions (MacSweeney et al. 2002; Emmorey et al. 2003). Prosody in sign language is transmitted via trunk and head posture as well as via facial expression (Sandler 2012) and its interpretation has been shown to activate predominantly right-hemispheric inferior frontal and superior temporal regions. Studies reporting recruitment of the classic fronto-temporal network in both spoken and signed language (MacSweeney et al. 2002; Leonard et al. 2012) further support the concept of modality-independence of the language network. These neuroscientific findings fit well into the concept of a domain-independent language system, and is aligned with the finding that spoken and signed languages exhibit similar linguistic characteristics such as recursive rule application and hierarchical structures (Lillo-Martin and Gajewski 2014).

Before spoken language can be understood, the speech signal has to be pre-processed by the hearer's bihemispheric auditory

Downloaded from https://academic.oup.com/cercor/article-abstract/30/2/812/5543064 by Charité - Med. Bibliothek user on 12 April 2020

system, requiring interhemispheric fiber bundles that support a direct exchange of information between the two hemispheres. Strong connections exist within the temporal cortex (Upadhyay et al. 2008), but also to the auditory cortex in the opposite hemisphere via commissural fibers through the presplenial and splenial part of the CC (Huang et al. 2005; Chao et al. 2009). These connections subserve the rapid interhemispheric transfer of auditory speech signals within the perceptual system and thus pave the way for successful comprehension of speech. This, in turn, is substantially influenced by auditory attention, employing mid-temporal as well as mainly right-hemispheric superior parietal and frontal areas (Zatorre et al. 1999).

Before sign language can be understood, visual information has to be processed in the visual system. Therefore, differences in speech networks between deaf and hearing participants are likely and have previously been investigated functionally and with regard to gray matter structural alterations. In a pioneering brain imaging study, Finney et al. (2001) revealed a partial takeover of auditory areas by the visual system in profoundly deaf individuals. Brain plasticity is also possible in the white matter, as indicated by structural magnetic resonance imaging (MRI) studies showing short-term as well as long-term learning-induced cortical changes in both gray and white matter (Draganski et al. 2004; Taubert et al. 2010; Schlegel et al. 2012).

In the present study, we investigate changes in white matter connectivity as a function of long-term use of sign language compared to spoken language. White matter pathways involved in the processing of acoustic information have been consistently found to be weaker in deaf signers compared to hearing controls, referring to fractional anisotropy (FA), a diffusion MRI (dMRI)-derived quantitative measure of brain microstructure (for a review see Tarabichi et al. 2018). Work focusing on subcortical tracts along the auditory pathway showed that participants with acquired hearing loss exhibit lower FA values in the lateral lemniscus and the inferior colliculus (Lin et al. 2008). Others revealed alterations in cortical white matter tracts such as the right SLF and inferior longitudinal fasciculus, corticospinal tract, inferior fronto-occipital fasciculus, superior occipital fasciculus, and anterior thalamic radiation (Husain et al. 2011). Studies including prelingually and congenitally deaf individuals reported lower FA values in bilateral superior temporal cortex and the splenium of CC in the deaf compared to the hearing group (Li et al. 2012; Karns et al. 2017; Kim et al. 2017). Lower FA points to reduced myelination, lower axonal density, a combination of both, or the presence of crossing fibers in the aforementioned regions, offering a variety of possible interpretations that cannot be construed with certainty (Jones et al. 2013).

The goal of the present study is to go beyond the auditory pathway and resolve the relation between the core language network and its connections to the auditory input and the motor output system necessary for speech processing. To this end, we compared prelingually deaf signers who learned GSL at an early age and could read and write German to a matched hearing control group. We employed dMRI-based probabilistic fiber tractography in order to analyze the connectivity profiles of six major language- and speech-associated areas in both hemispheres. This is a robust and well-established method to study brain connectivity, which provides a measure of the connection probability between a seed region and every voxel in the brain (Behrens et al. 2007). By examining the resulting seed-specific connectivity maps with voxel-based statistics, we were able to compare all connections of a selected region to their full extent and to localize connectivity differences between the two groups. This allowed us to separate speech-specific tracts from pathways of the core language system.

As described above, the core language system responsible for processing semantic and syntactic aspects of language is thought to be distinct from, but to functionally interact with a sensory-motor interface system during the perception and production of speech grounded in white matter pathways (Friederici et al. 2017). We distinguish two types of fibers that are relevant for our study. The first group covers fibers within the core language network, including the dorsally located SLF/AF targeting BA44 and the ventral pathway. The second type includes fibers belonging to the auditory input system as well as fibers belonging to the motor output system. This includes auditory areas and their interhemispheric fibers as well as motor output tracts targeting vBA6.

We anticipated differences in auditory-related white matter pathways involved in speech perception. With respect to the motor output system our expectations for differences were low, since speaking involves muscles similar to those employed in mouthing, an essential part of sign language. Based on the well-documented modality independence of the core language regions (Booth et al. 2002; MacSweeney et al. 2002; Emmorey et al. 2003; Patterson et al. 2007), we expected similar connectivity profiles of the core language pathways connecting BA44 and the posterior temporal cortex. These considerations guided our choice for the selection of seed regions of interest (ROIs) for probabilistic tractography and subsequent analyses. We defined seven ROIs in each hemisphere that served as seed masks for unidirectional probabilistic fiber tracking. These were six language-related ROIs located in BA44, vBA6, IPL, pSTG, pMTG, and HG as well as one control region in the visual cortex. As our goal was to unravel differences and similarities in connections beyond the classic language pathways, we did not define target, waypoint, and exclusion masks in order to compare all possible connections of the specific ROIs.

Materials and Methods

Experimental Design

The present study was designed to investigate the theory which assumes separate neural networks for language and speech. We compared white matter connectivity in hearing and deaf participants. These two groups were chosen, because they display similar language concepts, but communicate differently: exclusively via speech (hearing non-signers) or GSL (deaf signers).

Participants

Fifteen prelingually deaf adults were recruited for the study, but after application of strict inclusion parameters (see below), three among them had to be excluded from further participation. MR-data of 12 prelingually deaf adults who learned GSL within the first years of life and who could read and write German were acquired. Due to uncorrectable motion artifacts in one dataset and an incidental finding in another, only the data of 10 participants (mean age 31 years, range 25–39 years, three men) were analyzed (please see Table 1 for details). All participants were right-handed according to the Edinburgh Handedness Inventory (Oldfield 1971).

Participants of the deaf group had to express a high level of sign language proficiency and use GSL as their primary language of communication. All of them were diagnosed with

Downloaded from https://academic.oup.com/cercor/article-abstract/30/2/812/5543064 by Charité - Med. Bibliothek user on 12 April 2020

Table 1 Demographic data of all deaf participants

Age (y)	Sex	Cause of deafness	Age of onset of hearing impairment (y)	Age of onset of deafness (y;m)	Sign language use from age (y)	Hearing aid	Hearing loss of better ear[a] (dB)	Handedness	Mother/Father deaf
26	F	Unknown	0	2	3	No	94 (left)	Right	No/No
31	F	Rubella during pregnancy	0	0	3	Yes	125 (left)	Right	No/No
25	F	Unknown	0	0;7	6	Yes	109 (right)	Right	No/No
25	F	Unknown	0	0	3	Yes	94 (left)	Right	No/No
27	M	Ototoxic medication	-	1;6	3	No	124 (left)	Right	No/No
33	M	Hereditary	0	0	3	Yes	111 (left)	Right	No/No[b]
37	M	Hereditary	0	0	1	No	111 (left)	Right	Yes/Yes
39	F	Hereditary	0	0	3	No	114 (left)	Right	No/No
33	F	Unknown	0	0	3	No	116 (right)	Right	No/No
31	F	Hereditary	0	0	1	Yes	111 (right)	Right	Yes/Yes

[a]averaged over values at 500 Hz, 1000 Hz, 2000 Hz, and 4000 Hz, [b]Father knows GSL because of deaf grandmother.

sensorineural deafness, were fitted with hearing aids during early childhood and attended schools for deaf students. As there was no newborn hearing screening at the time the participants were born, we grounded our assessment on participants' self-reported history of deafness and other available medical documentation. According to this information, they were either born deaf or with severe progressing hearing impairment (with the exception of one participant who became deaf after receiving ototoxic medication at 1;6 years) so that they experienced deafness before the age of three in all cases. We only included participants with hearing thresholds above 90 dB on the better ear. In addition, their speech was examined by an experienced patholinguist. Those who used speech at a higher level than basic utterances were not included in our study. Pure tone audiometry results are averaged over hearing thresholds at 500 Hz, 1000 Hz, 2000 Hz, and 4000 Hz, because these frequencies best represent the range of spoken language. As 130 dB was the maximum possible stimulation threshold, values of tones that were not heard up to this level were set to 130 dB for averaging.

Ten control subjects (mean age 31 years, range 25–39 years, three men) were matched for sex, age, and handedness and received monetary compensation for their participation. All hearing participants were German native speakers with unremarkable tone audiograms and no knowledge of sign language. No participant reported having a history of neurological disorders or head injuries and all of them had normal neuroanatomy, which was confirmed by a neuroradiologist, who inspected all participants' MR images. After having been informed about risks and procedures, all participants gave written consent. The study was approved by the local Ethics Committee of the Faculty of Medicine at the Technical University of Dresden, and followed the ethical standards of the Helsinki Declaration.

Data Acquisition and Pre-processing of Diffusion Data

Anatomical and diffusion MR images were acquired with a 3 Tesla Tim-Trio MR-tomograph (Siemens Healthineers, Erlangen, Germany; software syngo MR B17) equipped with an eight-channel head coil. After obtaining a high-resolution structural T1-weighted scan, diffusion volumes were acquired with the following parameters: 60 gradient directions with a *b*-value 1000 s/mm^2 and 7 b0-volumes; 63 transversal slices without gap; twice-refocused echo-planar imaging sequence, interleaved recording; field of view 186 × 186 mm; voxel size 1.86 × 1.86 × 1.9 mm; repetition time 11.3 s and echo time 88 ms; 6/8 partial Fourier and GRAPPA 2 acceleration. After visual inspection and verification of absence of artifacts, data were motion corrected using rigid-body transformation computed with FSL (Jenkinson et al. 2002) (University of Oxford, UK, http://www.fmrib.ox.ac.uk/fsl) and linearly registered to the participants' individual T1 anatomy image in one combined step. The aligned diffusion image was masked with the brain mask obtained from the T1 image. Lastly, the diffusion tensor and FA maps were computed in every voxel. For the group analysis, all FA images were eroded and normalized to the FSL-FA template image using a linear and non-linear registration with default parameters (FSL's FLIRT and FNIRT) (Smith et al. 2006).

ROI definition

As depicted in Figure 1, we defined six ROIs in each hemisphere that served as seed masks for probabilistic fiber tracking. To investigate the auditory input system, we placed ROIs in bilateral HG. The ROIs covering the core language network were situated in BA44, pSTG, pMTG, and the central part of the IPL. To examine connections of the pre-motor output system, a ROI was placed in vBA6. Two additional ROIs in left and right primary visual cortex served as seeds for control tracts. The ROIs were drawn manually in ITK-SNAP (Yushkevich et al. 2006) on the FSL-FA-template (isotropic 1 mm resolution) based on anatomical landmarks. In order to separate tracks that start or end in the seed region from tracks that pass through it, we selected only the crown of the respective gyrus (50% of the local sulcal depth) and chose seed voxels at the gray matter/white matter boundary of each ROI in individual space.

The ROI in the pSTG was restricted posteriorly by the temporoparietal junction, superiorly by the Sylvian fissure, inferiorly by the superior temporal sulcus and anteriorly by the posterior border of HG. The latter as a whole was classified as HG ROI. We defined the pMTG ROI parallel to the one in pSTG with the superior temporal sulcus representing its superior border

Downloaded from https://academic.oup.com/cercor/article-abstract/30/2/812/5543064 by Charité - Med. Bibliothek user on 12 April 2020

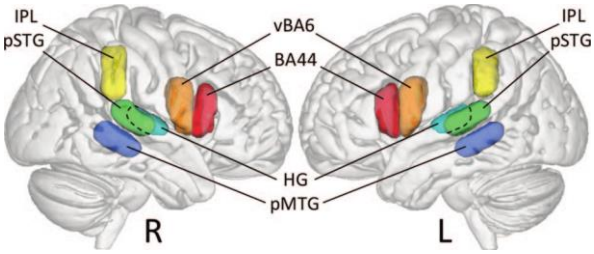

Figure 1. Seed ROIs for probabilistic tractography. Brodmann area 44 (BA44), ventral Brodmann area 6 (vBA6), central part of the IPL, pSTG, pMTG, and HG. HG is situated medial of pSTG and therefore marked with a dashed line. They do not overlap.

and the middle temporal sulcus the inferior one. Medially, all ROIs ended at the transition from gyrus to deep white matter. The ROI in BA44 was drawn over the opercular part of the IFG, with the Sylvian fissure and its anterior ascending ramus forming the inferior and the anterior borders, respectively. It was restricted posteriorly by the precentral sulcus, and its superior boundary was the inferior frontal sulcus. Posteriorly adjacent to BA44, we defined the precentral ROI in vBA6, which reached from the Sylvian fissure up to the IFS and had its posterior border at the central sulcus. The parietal ROI covered the central portion of the IPL posterior to the ascending branch of the Sylvian fissure and was restricted superiorly by the intraparietal sulcus and inferiorly by the temporoparietal junction (Ruschel et al. 2014). The control ROIs in the primary visual cortex were based on the Juelich histological atlas beyond 50% probability (Amunts et al. 2000).

All ROIs were smoothed with a spherical kernel of 2 mm and aligned to each participant's FA images by applying the inverse normalization steps computed in the previous normalization of the individual FA images to the FSL-FA template (Smith et al. 2006). As we intended to start probabilistic tracking at the transition from gray to white matter, the aligned ROIs were masked with participants' individual FA maps at a threshold of 0.15, providing a white matter mask. After removing disconnected voxels left by the masking process, we selected only the white matter border voxels of the resulting ROIs as seed regions. The transition of the FA values between white and gray matter is smooth at the chosen resolution of the diffusion images. An FA threshold of 0.15 provides a white matter mask that might include boundary voxels with a partial volume of gray matter at its borders as revealed by a direct comparison with the segmentation of the high resolution T1 image. This relatively low threshold was chosen to robustly seed the tractography only at the white matter/gray matter boundary. After each step, the ROIs were carefully checked and, if necessary, adjusted to ensure proper alignment. Supplementary Table S1 summarizes the final sizes of all seed ROIs. Note that the applied FA threshold for the seed voxels should not be confused with any threshold applied during the tractography process. Probabilistic tracking was conducted employing a whole brain mask instead of a white matter mask.

Probabilistic Tractography

In preparation for probabilistic tracking, we computed the fiber orientation distribution for every voxel with FSL's BEDPOSTX (Behrens et al. 2007) software. Up to two fiber orientations were modeled in each voxel, which were used for the computation of tracking directions. Probabilistic tracking was performed unidirectionally from each of the 14 seed ROIs separately for every participant. As our goal was to unravel the differences and similarities in connections beyond the classic language pathways and to reduce unequal biases between participants, we did not include any target, waypoint, or exclusion masks. We used FSL PROBTRACKX (Behrens et al. 2007) with default parameters (5000 sample tracts per seed voxel, step length of 0.5 mm, curvature threshold of 0.2, maximum of 2000 steps per streamline, volume fraction threshold of subsidiary fiber orientations of 0.01). As the range of PROBTRACKX output images covered several orders of magnitude, we applied a logarithmic transform to each of the resulting tractography visitation maps to reduce the dynamic range. The transformed maps were then scaled with the log of the total number of streamlines as a function of the seed ROI's size to account for ROI size differences between participants. The resultant individual maps were normalized to the FSL-FA template in MNI space (1 mm isotropic) using the linear and non-linear normalization matrices and maps computed by normalizing the FA images as described before (Smith et al. 2006). The maps were then submitted to voxel-based statistics implemented in SPM12 (Wellcome Trust Centre for Neuroimaging; http://www.fil.ion.ucl.ac.uk/spm).

Apart from the normalization process, which implies a certain degree of smoothing, tractography images were not additionally smoothed. One reason for this approach is that the high resolution FA-based maps used for normalization are less prone to misalignments during registration compared to T1 images, as they provide a sharp white matter definition with high FA values in the centre of each gyrus. Secondly, we were interested in examining focal effects along the pathways. As these can be small in diameter and display some twists and curves along their trajectories, smoothing would erase their fine structure.

Statistical Analysis

The number of computed trajectories per voxel is indicative of the tractography's statistical precision and is influenced by the coherence of the analyzed white matter pathway. This measure relates indirectly to the white matter connectivity of the seed region. We compared the normalized connectivity maps between the two groups of participants to detect areas with reduced connection probability with respect to each seed ROI (Neef et al. 2018). For this statistical analysis, we applied a two-sample t-test (one-tailed) with default parameters in SPM. Areas with low and improbable connectivity values were masked by an explicit mask. For this purpose, we created an average scaled and normalized tractogram of all subjects in MNI-space and masked out regions with values lower than 0.2. For purposes of clarity, we used these average tractograms of all participants for visualization. All results were obtained using an uncorrected *P*-value of 0.005 at voxel level, a family wise error (FWE)-corrected *P*-value of 0.05 at cluster level and a cluster extent threshold of 100 voxels. All contrasts were calculated with $n = 20$.

Post hoc Analyses

Since the absence of a group effect is no evidence for similarity, we calculated interaction effects and Bayes Factor (Nieuwenhuis

Downloaded from https://academic.oup.com/cercor/article-abstract/30/2/812/5543064 by Charité - Med. Bibliothek user on 12 April 2020

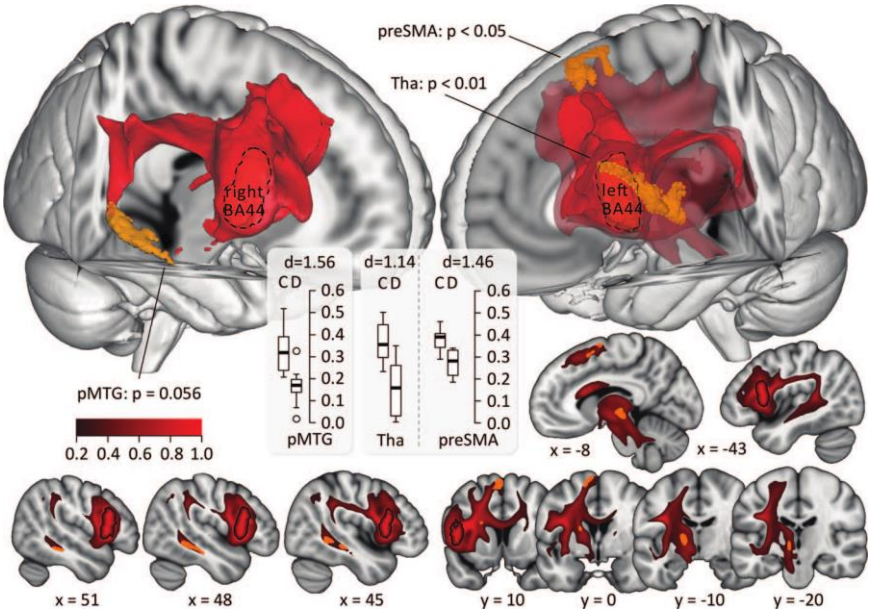

Figure 2. Tractography results with seed in Brodmann area 44 (BA44). Average tractograms of all participants are displayed on the standard T1 MNI-brain. Seed ROIs are marked with dashed lines. Tha, preSMA, and pMTG, where connectivity differed significantly between groups are depicted in orange (pMTG: trend). Color coding in slices ranges from 0 (no connectivity with seed ROI) to 1 (maximal connectivity). Tracts are shown at a threshold of 0.2, which was also used for statistical testing. For purposes of clarity, the tracts in the 3D images are presented at a threshold of 0.3. 3D images and horizontal slices are viewed from above and coronal slices from behind with left in the pictures representing left in the brain. Boxplots indicate mean logarithmized connectivity values of controls (C) and deafs (D) in areas with significant connectivity differences; Cohen's *d* was calculated post hoc. *P*-values are FWE-corrected at cluster level. All coordinates are given in MNI-space.

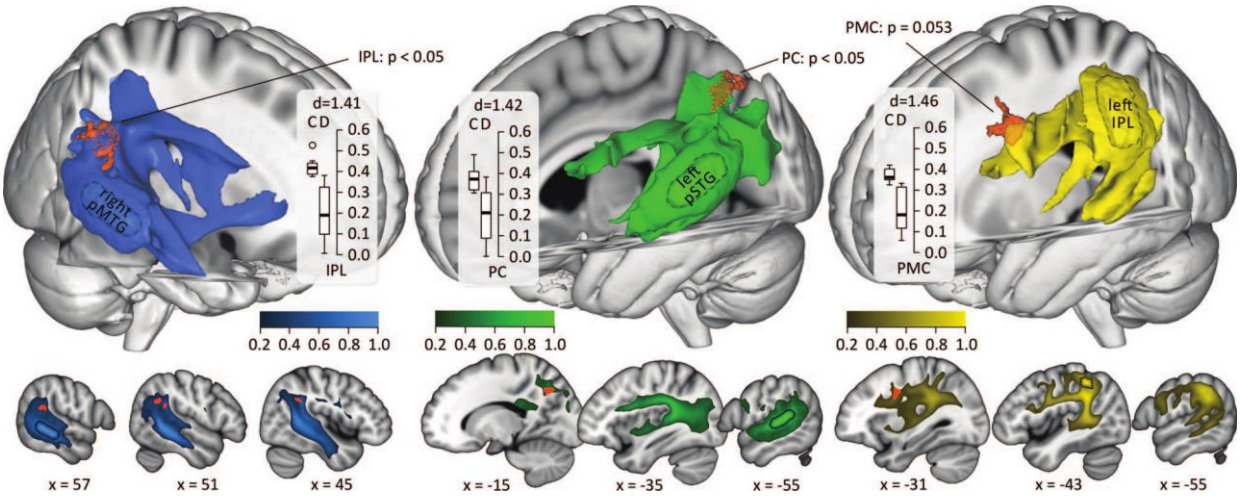

Figure 3. Tractography results with seeds in right pMTG (blue), left pSTG (green) and left IPL (yellow). Average tractograms of all participants are displayed on the standard T1 MNI-brain. Seed ROIs are marked with dashed lines. Right IPL, left precuneus (PC) and left premotor cortex (PMC), where connectivity differed significantly between groups (PMC: trend) are depicted in orange. Color coding in slices ranges from 0 (no connectivity with seed ROI) to 1 (maximal connectivity). Tracts are shown at a threshold of 0.2, which was also used for statistical testing. For purposes of clarity, the tracts in the 3D images are presented at a threshold of 0.3. Sagittal slices show left hemisphere for negative x and right hemisphere for positive x. Boxplots indicate mean logarithmized connectivity values of controls (C) and deafs (D) in areas with significant connectivity differences; Cohen's *d* was calculated post hoc. *P*-values are FWE-corrected at cluster level. All coordinates are given in MNI-space.

et al. 2011; Wetzels et al. 2011) in R (R Core Team 2016) for two tracts: the FAT representing the speech production network and the AF as part of the core language network. To this end, we selected the significant region in the left preSMA (please see results) and defined a similar region in the left posterior temporal cortex by defining a sphere around the two original seed ROIs in pMTG and pSTG. We chose these two regions in order to directly compare AF and FAT with respect to their targets when starting tractography in BA44. We masked the original connectivity maps with a mean map of all participants at a threshold of 0.2 to exclude improbable results. Within this map we extracted mean connectivity values for the significant region in the preSMA and for the previously defined region in the posterior temporal cortex. Calculation method and

Downloaded from https://academic.oup.com/cercor/article-abstract/30/2/812/5543064 by Charité - Med. Bibliothek user on 12 April 2020

Table 2 Results of probabilistic tractography

Seed	Connectivity difference in	Cluster size	Cluster p (FWE-corrected)	Peak T	Peakcoordinates (mm)			Mean connectivity		Effect size (Cohen's *d*)
					x	*y*	*z*	controls	deaf	
Left BA44	Left preSMA	673	0.024	4.36	−2	10	65	0.37	0.16	1.46
Left BA44	Left Tha	1001	0.003	4.11	−16	−4	14	0.38	0.28	1.14
Right BA44	Right MTG	490	0.056	4.93	47	−40	−7	0.33	0.16	1.56
Left HG	CC	2296	0.000	4.39	5	−31	17	0.38	0.18	1.38
Left HG	Left precuneus	671	0.013	4.39	−19	−60	37	0.47	0.25	1.27
Right HG	CC	1146	0.000	5.73	−18	−33	38	0.37	0.16	1.50
Left IPL	Left PMC	368	0.053	4.66	−30	−2	38	0.37	0.19	1.46
Left pSTG	Left precuneus	422	0.037	4.49	−14	−66	41	0.37	0.20	1.42
Right pMTG	Right IPL	539	0.023	4.47	45	−46	30	0.42	0.21	1.41

Note: HG: Heschl's gyrus; IPL: inferior parietal lobule; pSTG/pMTG: posterior superior/middle temporal gyrus; preSMA: pre-supplementary motor area; PMC: premotor cortex

nomenclature for the Bayes Factor are taken from the paper by Wetzels et al. (2011).

Data Availability

In alignment with the data protection clause in the ethics protocol which governed this study, data are available in non-identifiable format upon request. All analyses were conducted in FSL and SPM and are described above. No custom algorithms were used for analysis.

Results

Core Language Network

We reliably found the SLF/AF in both groups, confirming that our ROIs were placed appropriately. The different components of this pathway could be tracked bilaterally in both directions seeding frontally in BA44 (Fig. 2) and vBA6 (see Supplementary Fig. S1) as well as temporally in pMTG and pSTG (Fig. 3 and Supplementary Fig. S2). We detected no significant group differences for these fiber tracts. The IPL ROIs (Fig. 3 and Supplementary Fig. S2) also connected to frontal and temporal cortices via the short segments of the SLF/AF (Catani et al. 2005) in both hemispheres. This core pathway of the language network in the left hemisphere was not affected by early deafness and appeared to be similar in both groups. The ventral connections of the posterior temporal and the IPL ROIs towards the frontal lobe (Fig. 3 and Supplementary Fig. S2) did not display significant group differences.

Speech Perception and Production Network

We detected a number of pathways with significantly lower connection probability in the deaf group compared to the control group. These tracts are associated not with language processing in general, but with the production and perception of speech in particular. The differences in connectivity spanned a volume of at least 100 adjacent voxels at an FWE $P < 0.05$, corrected at cluster level. Pathways and regions with significant connectivity differences were smoothed for display in the sliced MR images. Effect sizes were calculated based on connectivity values in those regions with significant connectivity differences and were plotted with the corresponding MR images in standard space (Figs 2–4). Supplementary Tables S2–S8 provide a full list of results.

Speech Perception

The most striking group differences in the speech perception network appeared in the tracts seeded in bilateral HG, where both transcallosal connections (left-to-right and right-to-left) had significantly lower connectivity values in the deaf than in the control group (left: $P < 0.001$, right: $P < 0.001$; for details see Fig. 4 and Table 2). With regard to the left HG, the deaf group further showed a weaker continuation of the transcallosal connection towards the contralateral parietal and posterior temporal cortices. Moreover, the connections of the left HG (Fig. 4; $P = 0.01$) and the left pSTG (Fig. 3; $P < 0.05$) towards the ipsilateral PC had significantly lower probabilities in the deaf group, similar to the tract between the right pMTG and the right IPL (Fig. 3; $P < 0.05$).

Speech Production

Concerning speech production, tractography revealed significantly lower connectivity values for the left Broca–Tha–preSMA loop in the deaf group (Fig. 2; BA44 to preSMA: $P < 0.05$, BA44 to Tha: $P < 0.005$). Though only apparent as a trend ($P = 0.053$), the left IPL and the left PMC had a lower connection probability in the deaf than in the hearing group, strengthening this finding (Fig. 3). With regard to the right BA44 as seed ROI, we observed a trend to lower connectivity with the ipsilateral pMTG in the deaf group (Fig. 2; $P = 0.056$).

In order to test for a dissociation of a core language network and an output system for speech processing, we directly compared AF and FAT with respect to their targets when starting tractography in BA44 (Fig. 5). A repeated measures ANOVA with the between-groups factor "hearing status" and the within-groups factor "tract" revealed a significant interaction between "hearing status" and "tract" ($F_{1,36} = 11.471$, $P = 0.0017$) and a significant main effect of "hearing status" ($F_{1,36} = 13.232$, $P = 0.0009$). There was no main effect of the factor "tract" ($F_{1,36} = 0.431$, $P = 0.52$). Pairwise post hoc comparisons (corrected for multiple comparisons; Holm 1979) showed that the main effect "hearing status" was driven by the group difference in the FAT ($P = 0.0013$, one-tailed), while the groups' means did not differ in the AF ($P = 0.41$, one-tailed). These findings were corroborated by their respective Bayes Factor. We found very strong evidence for the group difference in the FAT ($BF_{A0} = 59.39$). The Bayes Factor for the AF was $BF_{0A} = 3.17$, providing substantial evidence for similarity. Additionally, we reconstructed control tracts from visual seed ROIs and found similar trajectories in both groups without significant differences.

Downloaded from https://academic.oup.com/cercor/article-abstract/30/2/812/5543064 by Charité - Med. Bibliothek user on 12 April 2020

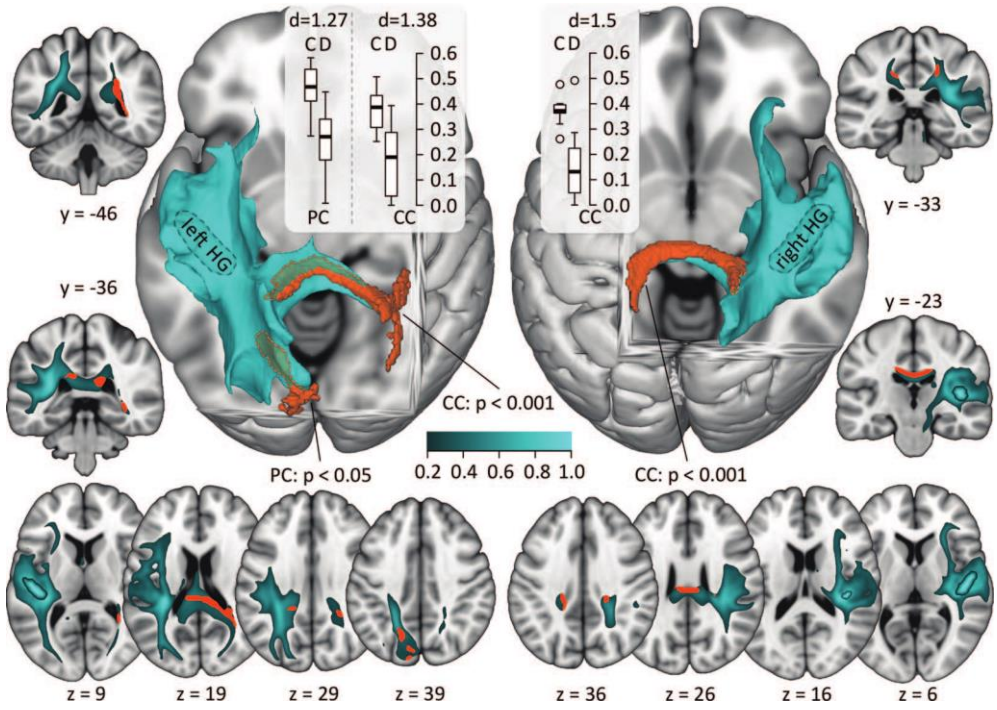

Figure 4. Tractography results with seed in HG. Average tractograms of all participants are displayed on the standard T1 MNI-brain. Seed ROIs are marked with dashed lines. CC and left PC, where connectivity differed significantly between groups are depicted in orange. Color coding in slices ranges from 0 (no connectivity with seed ROI) to 1 (maximal connectivity). Tracts are shown at a threshold of 0.2, which was also used for statistical testing. For purposes of clarity, the tracts in the 3D images are presented at a threshold of 0.3. 3D images and horizontal slices are viewed from above and coronal slices from behind with left in the pictures representing left in the brain. Boxplots indicate mean logarithmized connectivity values of controls (C) and deafs (D) in areas with significant connectivity differences; Cohen's *d* was calculated post hoc. *P*-values are FWE-corrected at cluster level. All coordinates are given in MNI-space.

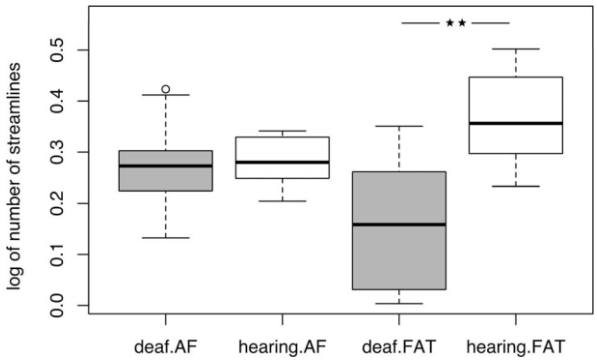

Figure 5. Connectivity values in the left FAT seeded in BA44 and targeting the preSMA and the left AF seeded in BA44 and targeting posterior temporal cortex. Boxplots indicate mean logarithmized connectivity values of deaf (gray) and hearing (white) participants in AF and FAT with a significant group difference in the FAT ($P = 0.0013$, one-tailed) and no significant group difference in the AF ($P = 0.41$, one-tailed). *P*-values are corrected for multiple comparisons. Asterisk indicates significance at $^{**}P < 0.01$.

Discussion

Using a novel approach for analyzing probabilistic tractography group differences, we were able to disentangle white matter pathways involved in speech processing from those subserving language itself. This finding provides structural evidence for the theoretically-proposed segregation of a core language system and input/output systems responsible for externalization (Friederici et al. 2017). We reliably found the major dorsal language tract, which is the SLF/AF targeting BA44, in both groups, underlining the general modality-independence of the core language network (MacSweeney et al. 2002), further supported by similar connection probabilities in the ventral language pathway of both deaf and hearing participants. In contrast, regions of the sensory-motor system involved in the production and perception of speech had significantly lower connectivity values in the deaf group compared to the hearing group, indicating their modality dependency. Moreover, producing and understanding spoken language is claimed to rely on fast feedback mechanisms between the core language network and the speech network, including the (sub)cortical motor system, oropharyngeal muscles and the hearing system (Dick et al. 2014). In prelingually deaf individuals, these input/output related circuits do not seem to be equally well established. The present results call for a fine-grained discussion of BA44 region's role in the core language system and its relation to the sensory-motor system, including subcortical parts of the production networks. Before doing so we will consider the perception network involving the left and the right hemisphere.

Concerning circuits subserving speech perception, there exists a general scientific consensus with regard to the identification of degraded subcortical auditory pathways in deaf individuals (Lin et al. 2008; Tarabichi et al. 2018). In this study, we built on previous results (Li et al. 2012) by showing that the callosal connection between the auditory cortices appears to

Downloaded from https://academic.oup.com/cercor/article-abstract/30/2/812/5543064 by Charité - Med. Bibliothek user on 12 April 2020

be weakened in prelingually deaf individuals. This connection seems to be crucial for a rapid transfer of acoustic information processed in both hemispheres at an early cortical processing stage, as indicated by white matter changes in the splenial CC of professional interpreters (Elmer et al. 2011). They rely on the fast integration of interhemispheric computational differences (Hickok and Poeppel 2007) with the left auditory cortex being more responsive to high-temporal (segmental) changes in speech signals and the right one to spectral (supra-segmental) variations (Zatorre and Belin 2001). Furthermore, our analyses yielded lower connectivity between the left HG and contralateral parietal as well as midtemporal cortices. This connection provides a structural basis for the interhemispheric interaction needed for sentence-level auditory prosody processing with a commissural connection that directly links the primary auditory cortex to contralateral higher-order integration areas (Friederici et al. 2007). The identification of less developed pathways for auditory prosody processing in our study's deaf participants was complemented by lower connection probabilities between the right MTG seed and the IPL as well as between the right BA44 seed and the MTG. This finding underlines the role of these tracts in the processing of speech (Price 2012).

Apart from transferring prosodic speech information (Friederici et al. 2007), the splenium of the CC is known to be crucial for attention-demanding tasks in the auditory, visual, and tactile domains with the right hemisphere outperforming the left one (Dimond 1979). The missing auditory attention capacities of the deaf group may have further contributed to the reduced transcallosal connectivity of the auditory cortices. Although some auditory features such as tonotopic functional connectivity seem to be preserved to varying degrees in severely hearing-impaired individuals (Striem-Amit et al. 2016), the connections described above might not be completely established in such individuals. They may be diminished due to pruning processes in early childhood occurring in the context of auditory deprivation and/or due to the later lack of use.

Deafness is not only about hearing and speech perception, but also about producing speech. The neural network that is responsible for speech production encompasses motor as well as somatosensory and auditory regions involved in feedback loops for real-time adjustment of articulatory output (Price 2012). One of the tracts that seems to be associated with producing fluent speech is the FAT between left BA44/vBA6 and preSMA/SMA, two regions crucial for speech initiation (Price 2012; Catani et al. 2013; Flinker et al. 2015). As the deaf participants in our study hardly communicate orally, this pathway may not have developed to its fullest possible extent. In the group comparisons of the BA44 connectivity profiles, the respective values of the FAT were lower in the deaf group, which highlights its importance for speech initiation and builds on the findings from a post-stroke aphasia study demonstrating FAT involvement in speech fluency (Halai et al. 2017).

The connection between the left BA44 and the Tha as part of the cortico-basal ganglia-thalamo-cortical circuit for motor processing of speech (Dick et al. 2014) also showed reduced connection probability in the deaf group. This is in line with previous results (Lyness et al. 2014) and underlines our finding of weakened connections involved in speech production, owing to this projection's role in supporting phonological language processing. We argue in favor of this suggestion based on deaf signers' limited capability of auditory phonological processing. There is phonology in sign language, but note that it is based upon hand configuration, location and movement (Sandler 2012).

The present findings illustrates BA44's key role as integration node in the language and speech network. It covers syntactic processing via the SLF/AF between BA44 and the posterior temporal cortex (Friederici et al. 2006; Skeide et al. 2016) independent of modality, reflected in the two groups' similar SLF/AF connectivity profiles. Moreover, it plays a crucial part in speech planning and initiation. In this role, however, BA44 reveals lower connectivity values in the tracts towards the preSMA and the Tha in the deaf group. As described above, vBA6 is functionally distinct from BA44 (Flinker et al. 2015) and covers those regions in the precentral gyrus which are relevant for mouth and facial movements—crucial in sign language. As such, the two groups' similar connectivity profiles with regard to vBA6 may be explained by this region's relevance for both speaking and mouthing during signing.

The PMC has been implicated in auditory discrimination of speech sounds as well as in auditory-motor mapping of speech and is involved in speech repetition, articulation and phonological word learning (Price 2012; López-Barroso et al. 2013; Flinker et al. 2015). These functions strongly rely on one part of the SLF/AF, which connects temporoparietal regions to the PMC as part of the dorsal pathway (Saur et al. 2008). While we observed no differences in the long segment of this pathway connecting the left temporal seed ROIs and BA44 known to be relevant for syntactic processes, the SLF's connectivity values between the left IPL seed and PMC were lower in the deaf group, emphasizing this part's role in auditory-motor integration during speech processing.

The connection between left supramarginal gyrus and PMC represents a key component of audiovisual speech processing that matures as experience in producing and perceiving spoken language increases (Dick et al. 2010). The lower connection probabilities we found in the deaf group are consistent with this model, because perceptional and articulatory deficits prevent audiovisual integration and further development of the respective pathways. As shown in an audiovisual fusion study, these pathways do not regrow after successful restoration of hearing with a cochlear implant (Schorr et al. 2005). Our results provide neuroanatomical underpinnings for these findings. In addition to this frontoparietal connection, the connectivity values between the left HG/pSTG seed and the ipsilateral PC extending to the intraparietal and parieto-occipital sulcus were significantly lower in the deaf group. These regions have been suggested to contribute to auditory-visual object recognition (for a review see Price 2012), completing the picture of a diminished fronto-temporo-parietal circuit for spoken language in the deaf group.

In order to obtain the results discussed above, we used probabilistic tractography. There are some methodological considerations concerning this technique. As it is an indirect measure of brain microstructure and connectivity, exact conclusions concerning the causes of the observed effects, such as changes in axonal diameter, myelinization, and fiber density cannot be drawn. Based on this indirect relation, connection probability is only a relative measure for actual connectivity. In this context, connectivity values serve as a correlate that can be compared between groups. Furthermore, dMRI is susceptible to measurement errors that may lead to the indication of inexistent connections or the negation of existing ones. It is important to note that, owing to sensitivity differences between the voxels close to a seed ROI and those voxels further away

Downloaded from https://academic.oup.com/cercor/article-abstract/30/2/812/5543064 by Charité - Med. Bibliothek user on 12 April 2020

from it, some connections may be detected in one tracking direction, but remain unidentifiable in the reverse one. We observed this effect in three regions: the left PMC, the left IPL, and the right MTG (Jones et al. 2013). Another methodological aspect to consider when interpreting the results is the limited sample size. This reduces the study's power and might have contributed to the absence of effects in some contrasts of our study. Here, further research with larger samples is needed in order to confirm and extend our results. However, taking into account existing fMRI research, strict selection procedures for participation in the current study, careful inspection of the data at all stages and the use of complex crossing fiber models (Behrens et al. 2007), we are confident that our results represent an important contribution to our understanding of the neural networks for speech and language.

Our findings of a preserved core language network paired with weaker tracts for speech processing in prelingually deaf signers certainly raise several issues. When studying deaf signing populations without a hearing signing control sample, it is not possible to clearly separate effects caused by auditory deprivation from those related to sign language use. Although we cannot directly compare our results to those of hearing signers, we interpret the observed effects in the context of auditory deprivation nevertheless. The reason for this is twofold. First, missing auditory input has a direct impact on the interhemispheric connections between the primary auditory areas, and this effect presumably occurs independently of sign language use. Second, all significant effects were reductions in the deaf group, pointing to tracts weakened by relatively low or no use. In the case of the pathways connecting the core language network with the sensory-motor system, the effects may be attributed to the absence of oral communication. This, in turn, is related to deafness and the lack of auditory feedback during speaking, but not to the use of sign language. Importantly, however, we ascribe the absence of connectivity differences in the core language pathways to early acquisition and use of sign language. These pathways appear to be equally developed in the deaf group, corroborating the concept of modality-independence of the core language network. Our study does not allow for conclusions about differential effects of early-onset as opposed to long-lasting deafness. Here, further research comparing prelingually deaf adults to long-term postlingually deaf participants is needed in order to disentangle developmental effects from the deterioration of pathways caused by long-lasting deafness.

Here, we showed that prelingual deafness paired with the early acquisition of sign language does not seem to affect the core language pathways, but may lead to changes in the connectivity of sensory and motor planning areas necessary for the processing of spoken language. The core language network seems to mature as long as either auditory or visual language input is provided in early childhood. In contrast, the pathways necessary for speech processing explicitly need auditory input and active speaking in order to mature to their full extent. Taken together, our findings demonstrate the modality-independence of the language network and provide structural evidence for the segregation of the core language system and speech processing circuits.

Supplementary Material

Supplementary material is available at *Cerebral Cortex* online.

Funding

German Research Foundation (grant number DFG/Ha 3153/2-1).

Note

We thank Alexander Mainka, Katrin Palisch and Stephan Schoebel for helping us with the recruitment of participants and we thank Steffi Heinemann for supporting the classification of the deaf participants' speech capacities.

Author's Contributions

AA, AH, ADF, DM, and JG designed the study; TF performed the research; TF and AA analyzed the data; TF, AA, AH and ADF wrote the paper.

References

Amunts K, Malikovic A, Mohlberg H, Schormann T, Zilles K. 2000. Brodmann's areas 17 and 18 brought into stereotaxic space—where and how variable? *NeuroImage*. 11:66–84.

Anwander A, Tittgemeyer M, von Cramon DY, Friederici AD, Knösche TR. 2007. Connectivity-based parcellation of Broca's area. *Cereb Cortex*. 17:816–825.

Bajada CJ, Lambon Ralph MA, Cloutman LL. 2015. Transport for language south of the Sylvian fissure: the routes and history of the main tracts and stations in the ventral language network. *Cortex*. 69:141–151.

Behrens TEJ, Berg HJ, Jbabdi S, Rushworth MFS, Woolrich MW. 2007. Probabilistic diffusion tractography with multiple fibre orientations: what can we gain? *NeuroImage*. 34:144–155.

Berwick RC, Friederici AD, Chomsky N, Bolhuis JJ. 2013. Evolution, brain, and the nature of language. *Trends Cogn Sci*. 17:89–98.

Booth JR, Burman DD, Meyer JR, Gitelman DR, Parrish TB, Mesulam MM. 2002. Modality independence of word comprehension. *Hum Brain Mapp*. 16:251–261.

Brauer J, Anwander A, Friederici AD. 2011. Neuroanatomical prerequisites for language functions in the maturing brain. *Cereb Cortex*. 21:459–466.

Catani M, Jones DK, Ffytche DH. 2005. Perisylvian language networks of the human brain. *Ann Neurol*. 57:8–16.

Catani M, Mesulam MM, Jakobsen E, Malik F, Martersteck A, Wieneke C, Thompson CK, Thiebaut de Schotten M, Dell'Acqua F, Weintraub S *et al*. 2013. A novel frontal pathway underlies verbal fluency in primary progressive aphasia. *Brain*. 136:2619–2628.

Chao Y-P, Cho K-H, Yeh C-H, Chou K-H, Chen J-H, Lin C-P. 2009. Probabilistic topography of human corpus callosum using cytoarchitectural parcellation and high angular resolution diffusion imaging tractography. *Hum Brain Mapp*. 30:3172–3187.

Dick AS, Bernal B, Tremblay P. 2014. The language connectome: new pathways, new concepts. *The Neuroscientist*. 20:453–467.

Dick AS, Garic D, Graziano P, Tremblay P. 2019. The frontal aslant tract (FAT) and its role in speech, language and executive function. *Cortex*. 111:148–163.

Dick AS, Solodkin A, Small SL. 2010. Neural development of networks for audiovisual speech comprehension. *Brain Lang*. 114:101–114.

Dimond SJ. 1979. Tactual and auditory vigilance in split-brain man. *J Neurol Neurosurg Psychiatry*. 42:70–74.

Draganski B, Gaser C, Busch V, Schuierer G, Bogdahn U, May A. 2004. Neuroplasticity: changes in gray matter induced by training. *Nature*. 427:311–312.

Downloaded from https://academic.oup.com/cercor/article-abstract/30/2/812/5543064 by Charité - Med. Bibliothek user on 12 April 2020

Elmer S, Hänggi J, Meyer M, Jäncke L. 2011. Differential language expertise related to white matter architecture in regions subserving sensory-motor coupling, articulation, and interhemispheric transfer. *Hum Brain Mapp*. 32:2064–2074.

Emmorey K, Allen JS, Bruss J, Schenker N, Damasio H. 2003. A morphometric analysis of auditory brain regions in congenitally deaf adults. *Proc Natl Acad Sci*. 100:10049–10054.

Finney EM, Fine I, Dobkins KR. 2001. Visual stimuli activate auditory cortex in the deaf. *Nat Neurosci*. 4:1171–1173.

Flinker A, Korzeniewska A, Shestyuk AY, Franaszczuk PJ, Dronkers NF, Knight RT, Crone NE. 2015. Redefining the role of Broca's area in speech. *Proc Natl Acad Sci*. 112:2871–2875.

Friederici AD, Bahlmann J, Heim S, Schubotz RI, Anwander A. 2006. The brain differentiates human and non-human grammars: functional localization and structural connectivity. *Proc Natl Acad Sci U S A*. 103:2458–2463.

Friederici AD, Chomsky N, Berwick RC, Moro A, Bolhuis JJ. 2017. Language, mind and brain. *Nat Hum Behav*. 1:713–722.

Friederici AD, von Cramon DY, Kotz SA. 2007. Role of the corpus callosum in speech comprehension: interfacing syntax and prosody. *Neuron*. 53:135–145.

Halai AD, Woollams AM, Lambon Ralph MA. 2017. Using principal component analysis to capture individual differences within a unified neuropsychological model of chronic post-stroke aphasia: revealing the unique neural correlates of speech fluency, phonology and semantics. *Cortex*. 86: 275–289.

Hagoort P, Indefrey P. 2014. The neurobiology of language beyond single words. *Annu Rev Neurosci*. 37:347–362.

Harris M, Beech JR. 1998. Implicit phonological awareness and early reading development in prelingually deaf children. *J Deaf Stud Deaf Educ*. 3:205–216.

Hickok G, Poeppel D. 2007. The cortical organization of speech processing. *Nat Rev Neurosci*. 8:393–402.

Holm S. 1979. A simple sequentially rejective multiple test procedure. *Scand J Stat*. 6:65–70.

Huang H, Zhang J, Jiang H, Wakana S, Poetscher L, Miller MI, van Zijl PC, Hillis AE, Wytik R, Mori S. 2005. DTI tractography based parcellation of white matter: application to the mid-sagittal morphology of corpus callosum. *NeuroImage*. 26:195–205.

Husain FT, Medina RE, Davis CW, Szymko-Bennett Y, Simonyan K, Pajor NM, Horwitz B. 2011. Neuroanatomical changes due to hearing loss and chronic tinnitus: a combined VBM and DTI study. *Brain Res*. 1369:74–88.

Jenkinson M, Bannister P, Brady M, Smith S. 2002. Improved optimization for the robust and accurate linear registration and motion correction of brain images. *NeuroImage*. 17:825–841.

Jones DK, Knösche TR, Turner R. 2013. White matter integrity, fiber count, and other fallacies: the do's and don'ts of diffusion MRI. *NeuroImage*. 73:239–254.

Karns CM, Stevens C, Dow MW, Schorr EM, Neville HJ. 2017. Atypical white-matter microstructure in congenitally deaf adults: a region of interest and tractography study using diffusion-tensor imaging. *Hear Res*. 343:72–82.

Kim J, Choi JY, Eo J, Park H-J. 2017. Comparative evaluation of the white matter fiber integrity in patients with prelingual and postlingual deafness. *NeuroReport*. 28:1103.

Leonard MK, Ramirez NF, Torres C, Travis KE, Hatrak M, Mayberry RI, Halgren E. 2012. Signed words in the congenitally deaf evoke typical late lexicosemantic responses with no early visual responses in left superior temporal cortex. *J Neurosci*. 32:9700–9705.

Li Y, Ding G, Booth JR, Huang R, Lv Y, Zang Y, He Y, Peng D. 2012. Sensitive period for white-matter connectivity of superior temporal cortex in deaf people. *Hum Brain Mapp*. 33: 349–359.

Lillo-Martin DC, Gajewski J. 2014. One grammar or two? Sign languages and the nature of human language. *Wiley Interdiscip Rev Cogn Sci*. 5:387–401.

Lin Y, Wang J, Wu C, Wai Y, Yu J, Ng S. 2008. Diffusion tensor imaging of the auditory pathway in sensorineural hearing loss: changes in radial diffusivity and diffusion anisotropy. *J Magn Reson Imaging*. 28:598–603.

López-Barroso D, Catani M, Ripollés P, Dell'Acqua F, Rodríguez-Fornells A, de Diego-Balaguer R. 2013. Word learning is mediated by the left arcuate fasciculus. *Proc Natl Acad Sci U S A*. 110:13168–13173.

Lyness RC, Alvarez I, Sereno MI, MacSweeney M. 2014. Microstructural differences in the thalamus and thalamic radiations in the congenitally deaf. *NeuroImage*. 100:347–357.

MacSweeney M, Woll B, Campbell R, McGuire PK, David AS, Williams SCR, Suckling J, Calvert GA, Brammer MJ. 2002. Neural systems underlying British Sign Language and audio–visual English processing in native users. *Brain*. 125:1583–1593.

Neef NE, Anwander A, Bütfering C, Schmidt-Samoa C, Friederici AD, Paulus W, Sommer M. 2018. Structural connectivity of right frontal hyperactive areas scales with stuttering severity. *Brain*. 141:191–204.

Nieuwenhuis S, Forstmann BU, Wagenmakers E-J. 2011. Erroneous analyses of interactions in neuroscience: a problem of significance. *Nat Neurosci*. 14:1105–1107.

Oldfield RC. 1971. The assessment and analysis of handedness: the Edinburgh inventory. *Neuropsychologia*. 9:97–113.

Patterson K, Nestor PJ, Rogers TT. 2007. Where do you know what you know? The representation of semantic knowledge in the human brain. *Nat Rev Neurosci*. 8:976–987.

Perani D, Saccuman MC, Scifo P, Anwander A, Spada D, Baldoli C, Poloniato A, Lohmann G, Friederici AD. 2011. Neural language networks at birth. *Proc Natl Acad Sci U S A*. 108: 16056–16061.

Petacchi A, Laird AR, Fox PT, Bower JM. 2005. Cerebellum and auditory function: an ALE meta-analysis of functional neuroimaging studies. *Hum Brain Mapp*. 25:118–128.

Price CJ. 2012. A review and synthesis of the first 20 years of PET and fMRI studies of heard speech, spoken language and reading. *NeuroImage*. 62:816–847.

R Core Team. 2016. *R: a language and environment for statistical computing*. R Foundation for Statistical Computing.

Ruschel M, Knösche TR, Friederici AD, Turner R, Geyer S, Anwander A. 2014. Connectivity architecture and subdivision of the human inferior parietal cortex revealed by diffusion MRI. *Cereb Cortex*. 24:2436–2448.

Sammler D, Grosbras M-H, Anwander A, Bestelmeyer PEG, Belin P. 2015. Dorsal and ventral pathways for prosody. *Curr Biol*. 25:3079–3085.

Sammler D, Cunitz K, Gierhan SM, Anwander A, Adermann J, Meixensberger J, Friederici AD. 2018. White matter pathways for prosodic structure building: a case study. *Brain Lang*. 183:1–10.

Sandler W. 2012. The phonological organization of sign languages. *Lang Linguist Compass*. 6:162–182.

Saur D, Kreher BW, Schnell S, Kümmerer D, Kellmeyer P, Vry M-S, Umarova R, Musso M, Glauche V, Abel S *et al*. 2008.

Downloaded from https://academic.oup.com/cercor/article-abstract/30/2/812/5543064 by Charité - Med. Bibliothek user on 12 April 2020

Ventral and dorsal pathways for language. *Proc Natl Acad Sci*. 105:18035–18040.

Schlegel AA, Rudelson JJ, Tse PU. 2012. White matter structure changes as adults learn a second language. *J Cogn Neurosci*. 24:1664–1670.

Schorr EA, Fox NA, van Wassenhove V, Knudsen EI. 2005. Auditory-visual fusion in speech perception in children with cochlear implants. *Proc Natl Acad Sci U S A*. 102:18748–18750.

Skeide MA, Brauer J, Friederici AD. 2016. Brain functional and structural predictors of language performance. *Cereb Cortex*. 26:2127–2139.

Smith RJ, Shearer AE, Hildebrand MS, Van Camp G. 1993. Deafness and hereditary hearing loss overview. In: Pagon RA, Adam MP, Ardinger HH, Wallace SE, Amemiya A, Bean LJ, Bird TD, Fong C-T, Mefford HC, Smith RJ, Stephens K, editors. *GeneReviews®*. Seattle (WA): University of Washington, Seattle.

Smith SM, Jenkinson M, Johansen-Berg H, Rueckert D, Nichols TE, Mackay CE, Watkins KE, Ciccarelli O, Cader MZ, Matthews PM *et al*. 2006. Tract-based spatial statistics: voxelwise analysis of multi-subject diffusion data. *NeuroImage*. 31:1487–1505.

Striem-Amit E, Almeida J, Belledonne M, Chen Q, Fang Y, Han Z, Caramazza A, Bi Y. 2016. Topographical functional connectivity patterns exist in the congenitally, prelingually deaf. *Sci Rep*. 6:29375.

Tarabichi O, Kozin ED, Kanumuri VV, Barber S, Ghosh S, Sitek KR, Reinshagen K, Herrmann B, Remenschneider AK, Lee DJ. 2018. Diffusion tensor imaging of central auditory pathways in patients with sensorineural hearing loss: a systematic review. *Otolaryngol Head Neck Surg*. 158: 432–442.

Taubert M, Draganski B, Anwander A, Müller K, Horstmann A, Villringer A, Ragert P. 2010. Dynamic properties of human brain structure: learning-related changes in cortical areas and associated fiber connections. *J Neurosci*. 30: 11670–11677.

Upadhyay J, Hallock K, Ducros M, Kim D-S, Ronen I. 2008. Diffusion tensor spectroscopy and imaging of the arcuate fasciculus. *NeuroImage*. 39:1–9.

Wetzels R, Matzke D, Lee MD, Rouder JN, Iverson GJ, Wagenmakers E-J. 2011. Statistical evidence in experimental psychology: an empirical comparison using 855 *t* tests. *Perspect Psychol Sci*. 6:291–298.

Yushkevich PA, Piven J, Hazlett HC, Smith RG, Ho S, Gee JC, Gerig G. 2006. User-guided 3D active contour segmentation of anatomical structures: significantly improved efficiency and reliability. *NeuroImage*. 31:1116–1128.

Zatorre RJ, Belin P. 2001. Spectral and temporal processing in human auditory cortex. *Cereb Cortex*. 11:946–953.

Zatorre RJ, Mondor TA, Evans AC. 1999. Auditory attention to space and frequency activates similar cerebral systems. *NeuroImage*. 10:544–554.

Zhang Y, Fan L, Caspers S, Heim S, Song M, Liu C, Mo Y, Eickhoff SB, Amunts K, Jiang T. 2017. Cross-cultural consistency and diversity in intrinsic functional organization of Broca's region. *NeuroImage*. 150:177–190.

Downloaded from https://academic.oup.com/cercor/article-abstract/30/2/812/5543064 by Charité - Med. Bibliothek user on 12 April 2020

5.2 Supplementary material

Theresa Finkl, Anja Hahne, Angela D Friederici, Johannes Gerber, Dirk Mürbe, Alfred Anwander, **Language Without Speech: Segregating Distinct Circuits in the Human Brain**, *Cerebral Cortex*, Volume 30, Issue 2, February 2020, Pages 812–823, https://doi.org/10.1093/cercor/bhz128, *online publiziert im August 2019*

Supplementary figures and tables to "Language without speech: Segregating distinct circuits in the human brain" (Finkl et al. 2020)

Formatting adjusted to fit the margins of this document.

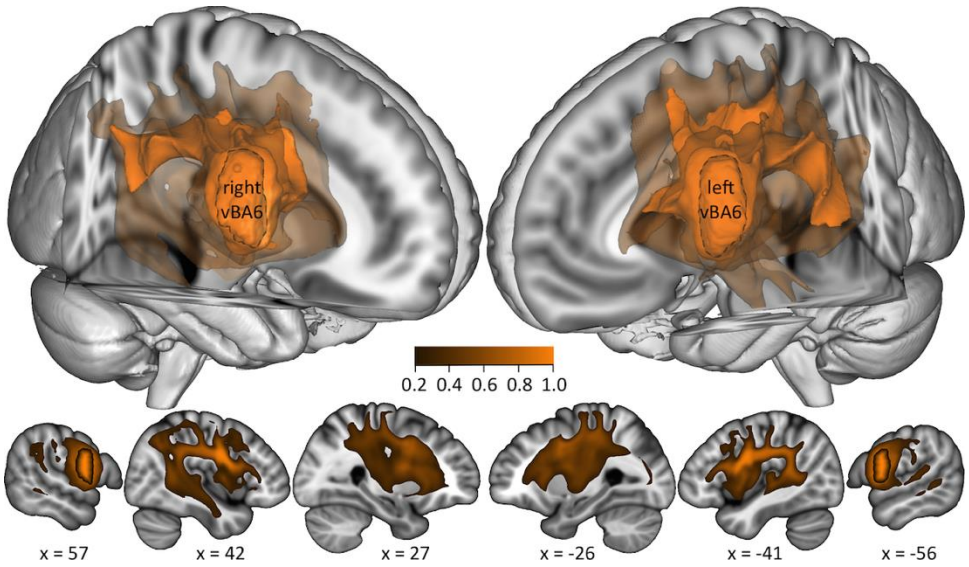

Figure S1) Tractography results with seed in ventral Brodmann area 6 (vBA6). Both groups had similar tracts without significant differences. Average tractograms of all participants are displayed on the standard T1 MNI-brain. Seed ROIs are marked with dashed lines. Color coding in slices from 0 (no connectivity with seed ROI) to 1 (maximal connectivity). Tracts are shown at a threshold of 0.2, which was also used for statistical testing. For purposes of clarity, the tracts in the 3D images are presented at a threshold of 0.3. Due to the broad connectivity of vBA6, the tractogram at 0.3 is transparent and an additional solid one at a threshold of 0.45 is overlaid. Sagittal slices show left hemisphere for negative x and right hemisphere for positive x. All coordinates are given in MNI-space.

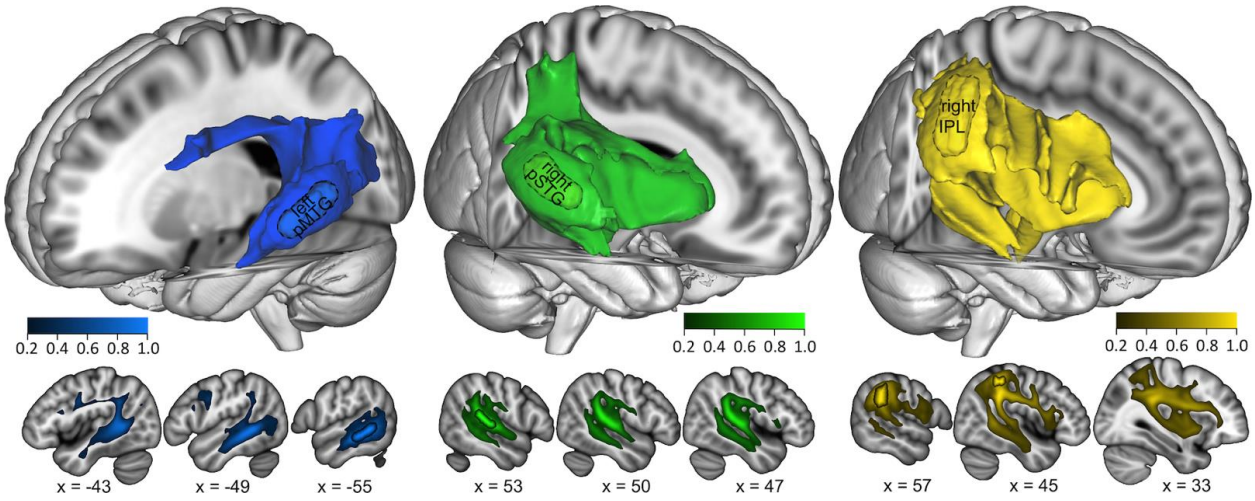

Figure S2) Tractography results with seeds in left posterior middle temporal gyrus (pMTG; blue), right posterior superior temporal gyrus (pSTG; green) and right inferior parietal lobule (IPL; yellow). Both groups had similar tracts without significant differences. Average tractograms of all participants are displayed on the standard T1 MNI-brain. Seed ROIs are marked with dashed lines. Color coding in slices from 0 (no connectivity with seed ROI) to 1 (maximal connectivity). Tracts are shown at a threshold of 0.2, which was also used for statistical testing. For purposes of clarity, the tracts in the 3D images are presented at a threshold of 0.3. Sagittal slices show left hemisphere for negative x and right hemisphere for positive x. All coordinates are given in MNI-space.

Table S1: Final sizes of all seed ROIs (number of voxels)

	Hearing participants										Mean		Deaf participants									
	C1	C2	C3	C4	C5	C6	C7	C8	C9	C10	hearing	deaf	D1	D2	D3	D4	D5	D6	D7	D8	D9	D10
BA44 L	226	135	159	224	174	269	161	185	190	288	201	190	192	183	147	150	268	202	183	186	198	190
BA44 R	160	166	141	185	165	215	167	167	103	176	165	184	248	163	165	161	185	222	228	109	182	179
vBA6 L	259	233	237	287	335	345	273	300	320	361	295	293	263	354	328	262	330	287	255	240	318	290
vBA6 R	291	252	231	300	292	327	276	315	255	248	279	292	254	317	247	271	279	362	299	245	305	336
IPL L	125	171	169	153	178	210	117	180	135	202	164	216	236	156	169	184	282	234	213	233	200	253
IPL R	153	198	163	255	161	253	150	139	129	179	178	185	172	182	193	180	231	192	170	207	181	146
pSTG L	187	165	160	153	136	149	120	143	155	192	156	164	156	180	189	145	139	217	191	139	155	128
pSTG R	164	157	147	206	179	225	130	168	160	195	173	164	135	168	184	115	176	218	182	123	150	190
pMTG L	120	256	153	192	149	172	98	165	157	141	160	159	212	152	229	146	95	188	124	165	151	132
pMTG R	150	174	175	212	195	212	148	163	148	185	176	157	193	117	158	105	190	176	144	186	137	162
HG L	120	74	70	77	88	121	107	97	55	123	93	88	72	102	53	86	117	87	79	74	77	134
HG R	104	68	79	73	74	104	72	124	84	147	93	76	67	77	79	61	68	109	64	81	76	80
V1 L	594	433	585	596	713	540	509	761	457	794	598	634	521	447	598	558	787	725	790	593	728	596
V1 R	904	631	694	887	766	667	705	731	678	900	756	762	639	646	750	567	1077	907	827	585	822	800

Color coding: darker color inidicates smaller ROI size

Table S2: Results of probabilistic tractography from BA44

connectivity difference in	cluster size	cluster p (FWE-corrected)	cluster p (uncorrected)	peak T	peak coordinates (mm) x	y	z
Seed BA44 L Controls > Deaf							
Caudate L		0.837	0.071	4.524	-1	11	14
				4.211	0	2	18
MFG L		0.937	0.108	4.426	-30	17	39
preSMA L		0.024	0.001	4.356	-2	10	65
				4.037	-7	-1	69
				3.748	-8	12	56
preSMA L		0.875	0.081	4.248	-8	-7	60
				3.705	-14	-5	55
Thalamus L		0.003	0.000	4.113	-16	-4	14
				4.043	-22	11	22
				3.990	-14	-11	6
Seed BA44 R Controls > Deaf							
MTG R	490	0.056	0.003	4.926	47	-40	-7
				4.778	50	-28	-15
				3.718	46	-17	-20
MFG R	335	0.195	0.010	4.550	46	12	46
				3.970	43	19	42
PrCG R	170	0.680	0.055	4.224	29	-2	40

MFG: middle frontal gyrus, preSMA: pre-supplementary motor area, MTG: middle temporal gyrus, PrCG: Precentral gyrus

Table S3: Results of probabilistic tractography from HG

connectivity difference in	cluster size	cluster p (FWE-corrected)	cluster p (uncorrected)	peak T	peak coordinates (mm)		
					x	y	z
Seed HG L Controls > Deaf							
CC	2296	0.000	0.000	4.388	5	-31	17
				4.380	12	-35	19
				4.035	20	-39	22
PC L	671	0.013	0.001	4.387	-19	-60	37
				4.238	-9	-81	44
				3.685	-15	-67	41
PC R	100	0.922	0.129	4.097	18	-58	37
SOG L	201	0.530	0.038	4.063	-22	-80	25
				3.319	-15	-83	31
pCing L	149	0.745	0.069	3.545	-9	-43	24
				3.422	-1	-40	20
				3.143	8	-43	19
Seed HG L Deaf > Controls							
Insula L	107	0.902	0.117	3.910	-26	-25	17
Seed HG R Controls > Deaf							
CC	1146	0.000	0.000	5.726	-18	-33	38
				5.236	-13	-28	33
				4.225	-6	-24	28
SPL R	174	0.441	0.036	4.729	24	-41	52
HG R	247	0.215	0.015	4.589	43	-36	22
				4.374	50	-33	18
				3.336	54	-25	16
TP R	109	0.758	0.087	4.446	63	-25	11
				3.189	56	-32	13
Thalamus R	299	0.128	0.008	4.302	22	-22	5
				4.250	15	-23	-2
				3.414	9	-28	-7

CC: corpus callosum, PC: precuneus, SOG: superior occipital gyrus, pCing: posterior cingulum, SPL: superior parietal lobule, HG: Heschl's gyrus, TP: temporal plane

Table S4: Results of probabilistic tractography from vBA6

connectivity difference in	cluster size	cluster p (FWE-corrected)	cluster p (uncorrected)	peak T	peak coordinates (mm)		
					x	y	z
Seed vBA6 L Controls > Deaf							
PoCG L	136	0.890	0.068	5.316	-13	-36	71
				3.701	-21	-35	69
Insula L	188	0.684	0.036	5.039	-32	14	18
SFG L	172	0.753	0.043	4.649	-9	-1	69
PrCG L	156	0.818	0.053	4.434	-25	-27	67
MFG L	104	0.967	0.106	4.205	-31	17	38
Seed vBA6 R Controls > Deaf							
PrCG R	161	0.768	0.044	5.673	31	-11	65
				4.207	29	-15	58
PrCG R	103	0.962	0.099	4.448	51	6	19
MFG R	171	0.724	0.039	4.342	45	15	40

PoCG: Postcentral gyrus, SFG: superior frontal gyrus, PrCG: precentral gyrus, MFG: middle frontal gyrus

Table S5: Results of probabilistic tractography from pMTG

connectivity difference in	cluster size	cluster p (FWE-corrected)	cluster p (uncorrected)	peak T	peak coordinates (mm)		
					x	y	z
Seed pMTG L Controls > Deaf							
PrCG L	130	0.562	0.052	4.612	-32	-1	37
Seed pMTG L Deaf > Controls							
MTG L	152	0.449	0.038	5.491	-47	-60	7
			1.000	2.663	-65	14	
Seed pMTG R Controls > Deaf							
IPL L	148	0.659	0.060	7.575	64	-51	-1
	539	0.023	0.001	4.657	45	-46	30
				4.541	52	-51	28
				4.294	56	-40	22

PrCG: precentral gyrus, MTG: middle temporal gyrus, IPL: inferior parietal lobule

Table S6: Results of probabilistic tractography from pSTG

connectivity difference in	cluster size	cluster p (FWE-corrected)	cluster p (uncorrected)	peak T	peak coordinates (mm)		
					x	y	z
Seed pSTG L Controls > Deaf							
PC L	422	0.037	0.002	4.488	-14	-66	41
				3.886	-6	-78	40
				3.696	-19	-61	36
STG L	124	0.709	0.063	4.242	-59	-12	-5
MFG L	130	0.677	0.057	4.015	-32	-1	35
				3.663	-27	7	36
post Cingulate L	137	0.640	0.052	3.577	-28	-41	16
				3.353	-22	-39	24
				3.306	-13	-35	20
Seed pSTG R Controls > Deaf							
MTG R	395	0.082	0.004	5.998	48	-22	-17
				4.656	50	-31	-15
				4.155	45	-15	-22

PC: precuneus, STG: superior temporal gyrus, MFG: middle frontal gyrus, pCing: posterior cingulum, MTG: middle temporal gyrus

Table S7: Results of probabilistic tractography from IPL

connectivity difference in	cluster size	cluster p (FWE-corrected)	cluster p (uncorrected)	peak T	peak coordinates (mm)		
					x	y	z
Seed IPL L Controls > Deaf							
MFG L	368	0.053	0.003	6.188	-30	-2	38
				4.306	-20	-1	45
				3.263	-28	9	36
Seed IPL L Deaf > Controls							
PoCG L	160	0.496	0.033	4.729	-52	-20	41
				3.200	-55	-12	43
Seed IPL R Controls > Deaf							
MTG R	239	0.378	0.017	4.960	52	-31	-14
				3.736	47	-16	-17
	136	0.817	0.061	4.039	31	-50	40
SPL R				3.062	40	-52	42
PrCG R	114	0.901	0.083	3.573	31	-6	42
				3.377	30	-14	42
				3.192	30	2	41

MFG: middle frontal gyrus, PoCG: postcentral gyrus, MTG: middle temporal gyrus, SPL: superior parietal lobule, PrCG: precentral gyrus

Table S8: Results of probabilistic tractography from V1

connectivity difference in	cluster size	cluster p (FEW-corrected)	cluster p (uncorrected)	peak T	peak coordinates (mm)		
					x	y	z
Seed V1 L Controls > Deaf							
PP L	0.961	114	0.073	4.315	-45	-12	-16
PC L	0.979	103	0.087	4.091	21	-63	13
Basal FB L	0.944	122	0.065	3.912	-15	-2	-15
				3.072	-10	5	-19
Seed V1 R Controls > Deaf							
Amygdala R	0.088	447	0.002	6.150	30	-4	-22
				4.431	26	-6	-14
LiG R	0.736	200	0.023	5.338	3	-87	-15
OP R	0.355	295	0.008	4.623	4	-101	7
				4.264	8	-98	17
				3.526	17	-102	-3
LiG R	0.611	228	0.017	4.567	34	-42	-7
				3.556	26	-44	-3
HG L	0.071	471	0.001	4.429	-39	-38	7
				4.414	-35	-60	12
				3.821	-33	-58	20
Basal FB L	0.274	324	0.006	4.165	-9	5	-15
				4.090	-1	8	-13
PC L	0.952	138	0.053	4.068	27	-63	27
				3.411	24	-71	27
aOrbG L	0.977	123	0.066	3.570	23	45	-8
				3.297	29	39	-1

PP: polar plane, PC: precuneus, FB: forebrain, LiG: lingual gyrus, OP: occipital pole, HG: Heschl's gyrus, aOrbG: anterior orbital gyrus

6 LEBENSLAUF

Mein Lebenslauf wird aus datenschutzrechtlichen Gründen in der elektronischen Version meiner Arbeit nicht veröffentlicht.

7 PUBLIKATIONSLISTE

Aug 2019	**Artikel „Language Without Speech: Segregating Distinct Circuits in the Human Brain“**; 2020; Finkl T, Hahne A, Friederici AD, Gerber J, Mürbe D, Anwander A; *Cerebral Cortex*, 30(2):812–823; Impact Factor 6,308; https://doi.org/10.1093/cercor/bhz128, *online publiziert August 2019*
Feb 2017	**Poster „Entwicklung des Sprachverstehens von erwachsenen CI-Trägern in den ersten vier Monaten nach Erstanpassung“;** Hahne A, Finkl T, Mürbe D; *20. Jahrestagung der Deutschen Gesellschaft für Audiologie in Aalen*
Sep 2016	**Poster „Sprache ohne Laut: Strukturelle Besonderheiten im Sprachnetzwerk von prälingual ertaubten Erwachsenen“**; Finkl T, Anwander A, Friederici AD, Gerber J, Mainka A, Mürbe D, Hahne A**;** *33. Jahrestagung der Deutschen Gesellschaft für Phoniatrie und Pädaudiologie in Regensburg*
Sep 2015	**Poster „Verständnis von Wörtern mit Vorlage bei prä- und postlingual ertaubten, erwachsenen CI-Trägern“**; Finkl T, Mürbe D, Hahne A; *32. Jahrestagung der Deutschen Gesellschaft für Phoniatrie und Pädaudiologie in Oldenburg*
Sep 2014	**Poster „Traktographie des Fasciculus arcuatus bei prälingual ertaubten Patienten“**; Finkl T, Anwander A, Friederici AD, Gerber J, Mainka A, Mürbe D, Hahne A; *31. Jahrestagung der Deutschen Gesellschaft für Phoniatrie und Pädaudiologie in Lübeck*
Sep 2014	**Poster „Tractography of the fasciculus arcuatus in prelingually deaf patients“**; Finkl T, Anwander A, Friederici AD, Gerber J, Mainka A, Mürbe D, Hahne A; *5. internationale Konferenz „Auditory cortex: Towards a Synthesis of Human and Animal Research“ in Magdeburg*
Juni 2014	**Poster „Tractography of the language network in prelingually deaf patients“**; Finkl T, Anwander A, Friederici AD, Gerber J, Mainka A, Mürbe D, Hahne A; *13. internationale Konferenz „Cochlear Implants and Other Implantable Technologies“ in München*
Sep 2010	**Poster „Maximize success or minimize failure: individual achievement orientation modulates responsiveness to positive or negative reinforcement“**; Rehe C, Augenstein J, Finkl T, Hinrichs H, Münte T, Flechtner H, Krauel K; *12. internationales neurobiologisches Symposium "Learning and Memory: Cellular and Systemic Views“ in Magdeburg*

8 DANKSAGUNG

Es ist geschafft! Ich danke allen, die mich in dieser gefühlten Ewigkeit begleitet, ermutigt, unterstützt, getröstet und ertragen haben!

An erster Stelle gilt mein Dank Dr. Anja Hahne für die Betreuung meiner Dissertation. Danke, dass du mich über all die Zeit begleitet, ermutigt und unterstützt hast. Ohne dich wäre diese Arbeit nicht fertig geworden. Prof. Dirk Mürbe danke ich ebenfalls für die Betreuung und das Vertrauen in meine Arbeit sowie die Möglichkeit zum Blick über den Tellerrand auf verschiedenen Fachtagungen.

Ich möchte mich beim Team des SCIC Dresden für Rat und Tat sowie die tolle Atmosphäre bedanken. Mein Dank geht insbesondere an Alexander Mainka, Katrin Palisch, Stephan Schöbel, Steffi Heinemann und Uta Neumeister für die Unterstützung bei der Probandenakquise und –klassifizierung sowie an Mario Fleischer, mit dem der Büroalltag nie langweilig wurde.

Mein großer Dank gilt auch Willy Mattheus, der mit Engelsgeduld und viel Verständnis zu allen möglichen und unmöglichen Zeiten dafür gesorgt hat, dass ich auch bei räumlicher Distanz arbeitsfähig war und die Technik funktionierte. Nicht zuletzt möchte ich mich bei allen Probandinnen und Probanden bedanken, die sich bereitwillig haben scannen lassen und ohne die diese Arbeit nie zustande gekommen wäre.

Ein Riesendankeschön geht an Niki Vavatzanidis. DANKE fürs Wegbereiten, für gemeinsames Rumnerden, fröhliches Bugspotting in diversen Skripten, Experimente in der Laborküche, gegenseitiges Motivieren und Gespräche über Hirn und Herz! Ohne dich hätte ich so manchmal das Handtuch geworfen.

Mein Dank gilt auch Prof. Angela D Friederici und der Abteilung für Neuropsychologie am MPI Leipzig für die anregenden Diskussionen und Denkanstöße. Ganz besonders möchte ich mich bei Dr. Alfred Anwander bedanken, der mich für die Traktographie begeistert, mich in die Methodik eingearbeitet und kontinuierlich unterstützt hat. Danke, dass du immer ein offenes Ohr für meine Fragen und Ideen hattest und ich so viel von dir lernen durfte!

Mein Dank gilt der FAZIT-STIFTUNG für finanzielle Unterstützung und große Geduld. Auch der Graduiertenakademie der TU Dresden möchte ich für das Stipendium danken, aber ganz besonders für alles was ich dort jenseits meines Dissertationsthemas lernen durfte. Ihr Angebot ist große Klasse! Dank Dr. Matthias Rudlof erlangte ich eine zentrale Erkenntnis auf dem Weg zum Ziel und entwickelte die Idee für ein zukünftiges Projekt.

Außerhalb des Arbeitsalltags haben mich viele Menschen durch diese Zeit getragen, von denen ich einigen besonders danken möchte:

Dem Schwarzen Schaf und all seinen wechselnden Bewohner*innen. Ihr wart und seid immer wieder mein Anker in Dresden und ein zentraler Grund dafür, dass ich so gerne an diese Zeit zurück denke! Meiner Familie: Danke dass ihr immer an mich glaubt und mein Fundament seid, egal was ich vorhabe und wie lang es dauert. Ihr seid die Besten! Und Jean-Eudes: Danke fürs Abheben und Erden, fürs In-der-Spur-halten und Großzügig-über-vieles-hinwegschauen, für Geduld und Unterstützung – und für die besten Crêpes!